

Charge-Transfer Versus Charge-Transfer-Like Excitations Revisited[†]

Barry Moore, II,[†] Haitao Sun,^{†,‡} Niranjan Govind,[§] Karol Kowalski,[§] and Jochen Autschbach*,[†]

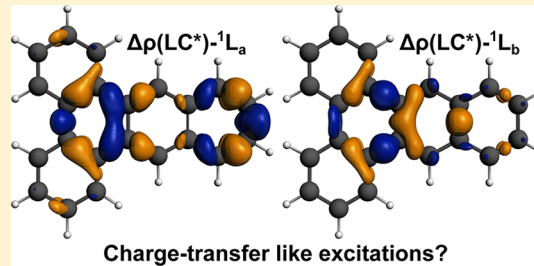
[†]Department of Chemistry, University at Buffalo, State University of New York, Buffalo, New York 14260-3000, United States

[‡]State Key Laboratory of Precision Spectroscopy, Department of Physics, East China Normal University, Shanghai 200062, P. R. China

[§]Environmental Molecular Sciences Laboratory, Pacific Northwest National Laboratory, Richland, Washington 99352, United States

S Supporting Information

ABSTRACT: Criteria to assess charge-transfer (CT) and CT-like character of electronic excitations are examined. Time-dependent density functional theory (TDDFT) calculations with non-hybrid, hybrid, and tuned long-range corrected (LC) functionals are compared with coupled-cluster (CC) benchmarks. The test set comprises an organic CT complex, two push–pull donor–acceptor chromophores, a cyanine dye, and several polycyclic aromatic hydrocarbons. Proper CT is easily identified. Excitations with significant density changes upon excitation within regions of close spatial proximity can also be diagnosed. For such excitations, the use of LC functionals in TDDFT sometimes leads to dramatic improvements of the singlet energies, similar to proper CT. It is shown that such CT-like excitations do not have the characteristics of physical charge transfer, and improvements with LC functionals may not be obtained for the right reasons. The TDDFT triplet excitation energies are underestimated for all systems, often severely. For the CT-like candidates, the singlet–triplet (S/T) separation changes from negative with a non-hybrid functional to positive with a tuned LC functional. For the cyanine, the S/T separation is systematically too large with TDDFT, leading to better error compensation for the singlet energy with a non-hybrid functional.



1. INTRODUCTION

In recent years, a number of theoretical studies have aimed to quantify the extent of charge-transfer (CT) in electronic excitations. For examples, see refs 1–6. The extent of CT character of electronic excitations is interesting in its own right, and its study is further motivated by the well-known breakdown of time-dependent (TD) density functional theory (DFT) linear response (LR) methods^{7–11} with standard adiabatic response kernels when applied to electronic CT excitation energies. For a transition involving predominantly just two orbitals, such as the highest occupied molecular orbital (HOMO, or H to keep the notation more compact) and the lowest unoccupied MO (LUMO, L), the TDDFT excitation energy can be grossly underestimated with non-hybrid and common hybrid functionals if the orbitals are spatially separated.^{2,9–17} Even for π to π^* transitions of organic chromophores that would normally not be assigned as CT, an ionic or CT-like character with a concomitant poor performance of TDDFT has been attributed to certain excitations.^{3,18–24} A lack of spatial overlap of the orbitals (vide infra) or the spatial separation of orbital centroids has been used to quantify the extent of CT or CT-likeness. For excitations where the transition density is described by a mixture of many occupied–unoccupied orbital pairs, weighted sums of such criteria have been employed. Linear-response TDDFT is at present the most frequently applied method for

calculating electronic spectra. Therefore, the CT problem and CT-like situations affect many research areas.

If there is a reliable diagnostic for CT, the user of a TDDFT program can then assess the likelihood of calculations being contaminated by the CT breakdown and take remedial measures or investigate further. Long-range corrected (LC) hybrid functionals using range-separated (RS) exchange have been designed to overcome the CT problem of TDDFT. Yanai et al.²⁵ pointed out that CT does not always involve spatially cleanly separated orbitals, in which case the performance of LC functionals is often not optimal, and a Coulomb-attenuated method (CAM) RS functional or a standard global hybrid may work better. An added complication with RS functionals is the choice of the parameters in the range-separation function, which critically affects the performance. A non-empirical molecule-specific determination of these parameters, via “tuning” of LC functionals and minimization of the DFT delocalization error^{3,11,26–34} (vide infra), often brings about the best performance in LC-TDDFT calculations of excitation spectra, but the procedure can be tedious and is not without shortcomings. Therefore, an assessment of the extent of CT or CT-like character of excitations remains an important topic, beyond assigning a spectrum.

Received: April 9, 2015

Published: June 1, 2015



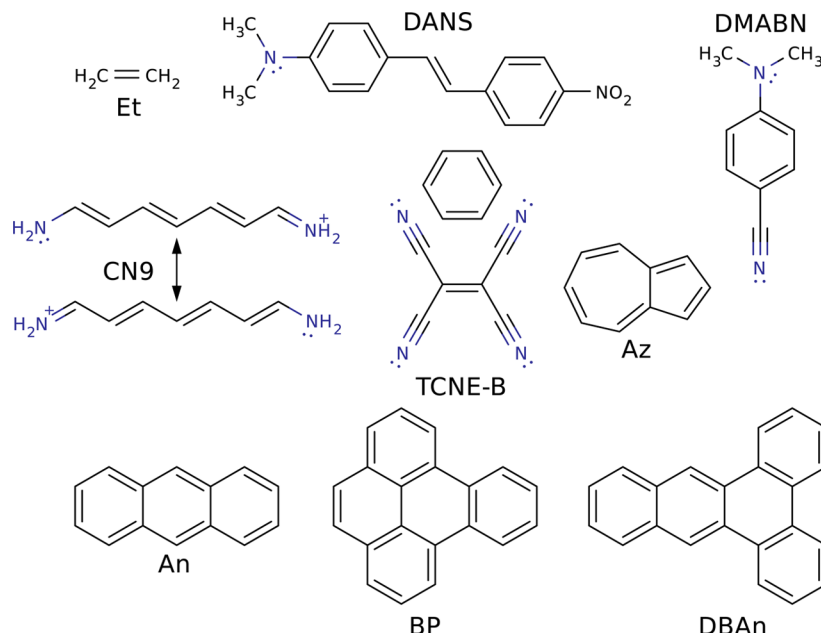


Figure 1. Molecules considered in this work. Acronyms used within the article: Et = ethene, DANS = 4-dimethylamino-4'-nitro-stilbene, DMABN = 4-dimethylamino-benzonitrile, CN9 = cyanine chromophore with a nine-atom backbone, Az = azulene, An = anthracene, BP = benzo[*e*] pyrene, and DBAn = dibenzobenzo[*a,c*] anthracene. TCNE-B is a coplanar tetracyanoethylene-benzene charge-transfer complex at $\sim 3.6 \text{ \AA}$ separation.

The present work is concerned with a comparison of different computational criteria for determining the CT character of an excitation and with the question of whether a CT-like situation can be identified reliably. The latter question is also interesting to ponder in its own right, by comparing different measures defined to assess CT and consider how the results relate to the physical extent of CT, which, to our knowledge, has no precise definition.

The set of organic chromophores considered in the present work is shown in Figure 1, along with shorthand names used in the remainder of the article. For this molecule set, TDDFT with standard functionals predicts some excitation energies well and others rather poorly. We focus on excitations with simple molecular orbital (MO) decompositions and investigate the magnitude of Coulomb and exchange integrals for the orbitals associated with the transitions, the magnitude of integrals of the DFT exchange-correlation (XC) response kernel with these orbitals, the magnitude of a combination of these integrals previously referred to as the CT term by Casida et al.,¹ various combinations of spatial orbital overlaps that were introduced previously for CT and CT-like diagnostics,³ and a recently proposed CT criterion based on orbital centroid distances.⁴ Further, we provide vertical singlet and triplet excitation energies from coupled-cluster (CC) and equation-of-motion coupled cluster (EOM-CC) calculations^{35–39} along with other wave function based data for comparison with TDDFT.

Clear-cut CT scenarios are easily identified, and the reasons for them causing problems in TDDFT are evident. The CT-like regime is less straightforward. We show that a previously devised criterion for CT-like cases has a diametrically opposed alternative interpretation for a two-level system and is not likely to indicate TDDFT problems due to an onset of physical CT. It is shown in this article that suboptimal performance of TDDFT and cases with potentially “right answers for the wrong reasons” within the set of chosen molecules can be linked to a systematic underestimation of triplet excitation energies combined with a gross over- or under-estimation of the energetic separation of

the singlet and triplet transitions (S/T gap) due to a poor description of differential correlation between the ground and the excited states. Section 2 provides computational details, Section 3 contains the results and discussion, and Section 4 summarizes the main conclusions.

2. COMPUTATIONAL DETAILS

Molecular structures for CN9 (MP2/cc-pVQZ),³⁴ BP and DBAn (B3LYP/6-31G*),¹⁸ and TCNE-B (B3LYP/cc-pVDZ)¹⁰ were taken from the literature (see citations for details). An and Az were optimized with Gaussian 09⁴⁰ using the B3LYP hybrid density functional^{41,42} and cc-pVTZ basis set,⁴³ following the details from ref 3. The other molecules were optimized using the B3LYP functional and 6-31G* Gaussian-type basis set.^{44,45} Molecular XYZ coordinates are provided in the Supporting Information.

Benchmark data for the vertical excitation energies were calculated with coupled-cluster (CC) methods, using completely renormalized (CR) equation-of-motion (EOM) CC for singlet excitation energies,⁴⁶ and differences of ground-state energies to obtain the energies of the triplet states relative to the singlet states. The CC calculations included singles and doubles (CCSD, CR-EOMCCSD), as well as singles and doubles with perturbative treatment of triples (CCSD(T), CR-EOMCCSD(T)), as implemented in NWChem, using the def2 triple- ζ valence polarized Gaussian-type basis⁴⁷ (available at the EMSL basis set exchange).⁴⁸ To reduce computational time a symmetrized DBAn structure was used for CC calculations (see Supporting Information for structure). DFT and TDDFT calculations of orbitals, excitation energies, and various CT criteria were performed with the TZVP basis as well, using a developer’s version of the NWChem package.^{49,50} The Perdew–Burke–Ernzerhof (PBE) generalized gradient approximation (GGA),⁵¹ the B3LYP global hybrid, and a tuned RS exchange hybrid functional based on PBE, were used. We also performed Hartree–Fock calculations. To facilitate functional tuning we employed a RS hybrid with a three-parameter error-

function separation of the interelectronic distance r_{12} as follows²⁵

$$\frac{1}{r_{12}} = \frac{1 - [\alpha + \beta \operatorname{erf}(\gamma r_{12})]}{r_{12}} + \frac{\alpha + \beta \operatorname{erf}(\gamma r_{12})}{r_{12}} \quad (1)$$

The long-range component of the hybrid functional is given by the second term on the right-hand side. The switching from DFT-like to (HF-like) exact exchange (eX) is determined by the range-separation parameter γ , representing the inverse of a distance around which the switching occurs. Ensuring a full long-range correction (LC, $\alpha + \beta = 1$), which is apparently needed for IP-tuning of isolated molecules,⁵² we used an LC-PBE variant with $\alpha = 0$, $\beta = 1$. The corresponding tuned versions with molecule-specific values of γ are labeled LC*. In this case, γ was determined to minimize

$$J^2 = \sum_{i=0}^1 [\epsilon_H(N+i) + \text{IP}(N+i)]^2 \quad (2)$$

Here, N is the electron number of the system, ϵ_H is the HOMO energy, and IP is the ionization potential calculated from self-consistent field (SCF) energy differences. The functionals were tuned using the 6-31+G* Gaussian-type basis set⁵³ for compatibility with our recent study of donor–acceptor CT chromophores,³³ which included DANS (Figure 1). In this previous paper, we also showed that the RS parameters tuned with 6-31+G* and TZVP are very similar. Applications of IP tuning have been discussed extensively in the literature; see, for example, refs 3,11,26,–29,31,–34. The procedure is designed such that ϵ_H is as close as possible to the negative IP, which is an exact condition in Kohn–Sham (KS) and generalized KS theory,^{27,54} for both the N -electron and $N+1$ electron systems. The procedure produces H–L energy gaps that are optimally close to the fundamental gap IP – EA of the N -electron system (EA is the electron affinity). In addition, the procedure often leads to functionals that exhibit a small DFT delocalization error, which can be minimized further.²⁸ The use of system-specific functionals is not recommended, for example, for thermochemistry,^{28,55,56} although their use in calculations of optimized structures and vibrational frequencies does not appear to be problematic.⁵⁷ Tuned LC functionals, optionally with quantification and minimization of the delocalization error, can be very useful for error diagnosis and in response calculations, and they may also improve ground-state electron densities and spin densities.⁵⁸

During the course of the project it became necessary to inspect the electron density differences between ground and excited states. The NWChem implementation for TDDFT LR excited-state gradients has been employed to obtain density differences between excited states and ground states (the excited-state gradient requires an extra step that gives access to various excited-state properties including the electron density).⁵⁹ Further, wave function calculations were performed with version 7.8 of the Molcas code⁶⁰ to compare the calculated difference densities with TDDFT. Here, the Gaussian-type basis set TZVP was used for C, N, O atoms, along with SVP⁴⁷ for hydrogens to reduce the computational effort. State-averaged complete active space self-consistent field (CASSCF) with inclusion of dynamical correlation by complete active space perturbation theory to second order (CASPT2) were performed as detailed in the Supporting Information, Tables S11 and S12.

For additional analyses of the excitations, a series of DFT calculations were performed with a locally modified version of the Amsterdam Density Functional (ADF) package,⁶¹ utilizing the TZ2P Slater-type basis set and the PBE functional. Various integrals were calculated for the frontier MOs using an ADF add-on previously developed to study TDDFT problems for 3d metal–ligand CT transitions and for π – π^* transitions of cyanines.^{16,34} The ADF add-on evaluates the integrals in the XC response kernel using the Vosko-Wilk-Nusair (VWN)⁶² local density approximation (LDA) functional. Electron repulsion integrals (ERIs) were calculated using the ‘twoel’ code included with ADF, which is a numerical integration code for two-electron integrals originally developed by Becke and Dickson that has been ported to recent ADF versions by one of us. The excitation energies for a two-level model assembled from the various integrals and the orbital energy gaps are in excellent agreement with corresponding NWChem PBE/TZVP two-level excitation energy calculations. For the latter, the TDDFT calculations excluded all but the H and L orbitals in the transition density by applying the “freeze” keyword.

Section 3.1 discusses various spatial overlap and density-based criteria for diagnosing CT and CT-like character of excitations. Numerical values for these criteria were obtained with a locally developed code for manipulating files containing volume data in the Gaussian cube format. Cube files for frontier canonical MOs and electron densities were created with NWChem and Molcas using grids of $101 \times 101 \times 101$ points extending 2 \AA beyond the lowest and highest coordinate values in the XYZ input molecular structures. Additionally, spatial overlaps were calculated for a set of four orbitals and general unitary transformations among them. An OpenMP parallelized code was written to perform large numbers of 4×4 unitary transformations of the MO volume data. To reduce the computational expense, the number of grid points was reduced to $51 \times 51 \times 51$. These software tools are available from the authors upon request.

3. RESULTS AND DISCUSSION

3.1. Criteria for Charge Transfer and Charge Transfer-Like Character of Excitations. In TDDFT, the linear response transition density matrix $\gamma_j^{(1)}(\mathbf{r}, \mathbf{r}')$ for an excitation number j is determined as a weighted sum of products of occupied (occ) and unoccupied (“virtual”, vir) canonical MOs ϕ_p , ϕ_q , and may be written as

$$\gamma_j^{(1)}(\mathbf{r}, \mathbf{r}') = \sum_i^{\text{occ}} \sum_a^{\text{vir}} [X_{i,a}^j \phi_i(\mathbf{r}') \phi_a(\mathbf{r}) + Y_{i,a}^j \phi_a(\mathbf{r}') \phi_i(\mathbf{r})] \quad (3)$$

The transition density is $\rho_j^{(1)}(\mathbf{r}) = \gamma_j^{(1)}(\mathbf{r}, \mathbf{r}' = \mathbf{r})$. Solving the TDDFT linear response equations gives the coefficient sets $X_{i,a}^j$, $Y_{i,a}^j$ for the transitions and the excitation energies E_j . Transition moments are calculated from the transition density (matrix). The orbitals are assumed to be real and orthonormal. Equation 3 allows for a convenient analysis and assignment of an excitation in terms of occ–vir pairs of MOs. The CT character of an excitation with a dominant contribution from an orbital pair can be assessed, for example, with the help of spatial overlaps.^{2,3,14,63} Among the suggested possibilities is the criterion

$$O_{p,q} = \langle |\phi_p| |\phi_q| \rangle = \langle |\phi_p \phi_q| \rangle = \int |\phi_p(\mathbf{r}) \phi_q(\mathbf{r})| dV \quad (4)$$

where $|\phi_p(r)| = [\phi_p(r)\phi_p(r)]^{1/2}$ is the absolute value of orbital ϕ_p (modulus). The notation $\langle \cdots \rangle$ is short for $\int \cdots dV$. The spatial overlap range is $0 \leq O_{p,q} \leq 1$.

A spatial overlap $O_{p,q}$ smaller than ~ 0.5 of an excitation that is dominantly assigned to an orbital pair ϕ_p, ϕ_q may indicate sizable long-range CT. The CT problem of TDDFT^{7–11} then usually leads to severely underestimated excitation energies in LR TDDFT calculations with non-hybrid functionals such as PBE (often to a lesser extent with hybrid functionals such as B3LYP), and incorrect trends regarding the chain-length dependence of band gaps of oligomers and donor–acceptor systems.^{2,30,33,64} RS functionals that switch to full eX at large interelectronic separations usually avoid this breakdown^{10,25,55,65} but may have to be tuned for a given molecule as described in Section 2 for best performance.^{26,58}

Recently, Guido et al. suggested another descriptor for the CT character of an excitation in TDDFT calculations. This descriptor is based on the distances between the centroids of pairs of orbitals such as $p = H, q = L$, involved in the excitation:⁴

$$\Delta r_{p,q} = |\langle \phi_p | \mathbf{r} | \phi_p \rangle - \langle \phi_q | \mathbf{r} | \phi_q \rangle| \quad (5)$$

A sum of $\Delta r_{p,q}$ weighted by the contribution of each orbital pair to the excitation vector was then used to assess CT character. A weighted sum of less than 1.5 Å was argued to indicate short-range excitations for which standard functionals are expected to perform reasonably well.

The valence π -to- π^* transitions of organic π -chromophores typically do not exhibit small $O_{p,q}$ and/or large $\Delta r_{p,q}$, but they may nonetheless afford a CT-like behavior in the sense that a too-low excitation energy may be improved noticeably by using a RS functional,^{18,66} in particular upon tuning.³ Kuritz et al.³ introduced a criterion to assess the occurrence of a CT-like (as opposed to CT) excitation as follows: Define a set of auxiliary orbitals:

$$\phi'_{p/q} = \pm(\phi_p \pm \phi_q)/\sqrt{2} \quad (6)$$

and calculate the spatial overlap $O'_{p,q} = O_{p',q'}$ with the auxiliary set using eq 4, for example, based on the H–L pair. It was pointed out that eq 6 is to be understood as a special case of a general orthogonal transformation of the two orbitals, parameterized by a rotation angle α :

$$\phi'_p(\alpha) = \phi_p \cos \alpha + \phi_q \sin \alpha \quad (7a)$$

$$\phi'_q(\alpha) = -\phi_p \sin \alpha + \phi_q \cos \alpha \quad (7b)$$

with the special case of eq 6, that is, $\alpha = \pm \pi/2$, being appropriate for symmetric molecules. According to Kuritz et al., general orthogonal transformations of two orbitals and the associated overlaps $O'_{p,q}(\alpha)$ may need to be considered for nonsymmetric molecules, and transformations among more than two orbitals may need to be considered for excitations involving large weights of several orbital pairs. For an excitation dominated by a single MO pair in a symmetric molecule, an “extreme charge-transfer-like” excitation was defined by Kuritz et al. as $O'_{p,q} = 0$. Consequently, small values of $O'_{p,q}$ have been associated with CT-like character in a $\pi-\pi^*$ transition, even for cases where $O_{p,q}$ is large. It was further argued that CT-like character could be present whenever a general orthogonal transformation among the participating orbitals leads to small spatial overlaps.

The centroid criterion eq 5 can also be applied to the transformed pair of eq 6, leading to

$$\Delta r'_{p,q} = 2|\langle \phi'_p | \mathbf{r} | \phi'_q \rangle| \quad (8)$$

Here, the result measures twice the geometrical average of the distances in x, y , and z direction over which the product $\phi'_p \phi'_q$ is nonzero, that is, a distance range over which ϕ_p and ϕ_q overlap.

As an example, in the acene series the ${}^1\text{L}_a$ (short-axis polarized, H–L) excitation energies are significantly underestimated by TDDFT calculations with non-hybrid Kohn–Sham potentials, whereas the ${}^1\text{L}_b$ excitations (long-axis polarized, mixing H–1–L and H–L+1 products) are predicted reasonably well. The use of RS exchange functionals improves the ${}^1\text{L}_a$ excitation energies. Numerical data (B3LYP) of the overlap criterion were provided in ref 3 for An: $O_{\text{H,L}} = 0.88$; $O'_{\text{H,L}} = 0.30$. The much smaller value of $O'_{\text{H,L}}$ compared to $O_{\text{H,L}}$ was identified as indicative for the poor performance of semilocal potentials due to a CT-like breakdown. Data for the orbitals participating in the ${}^1\text{L}_b$ excitation were not provided.

Before proceeding, we would like to elaborate on the $O'_{p,q}$ criterion. First, according to eq 6

$$\begin{aligned} O'_{p,q} &= \langle |\phi'_p| |\phi'_q| \rangle = \frac{1}{2} \langle |(\phi_p + \phi_q)(\phi_p - \phi_q)| \rangle \\ &= \frac{1}{2} \langle |\phi_q^2 - \phi_p^2| \rangle \end{aligned} \quad (9)$$

Using the general unitary transformation (7) of two orbitals involved in an excitation, the spatial overlap of the transformed pair becomes

$$\begin{aligned} O'_{p,q}(\alpha) &= \langle |\phi'_p \phi'_q| \rangle \\ &= \langle |(\phi_p \cos \alpha + \phi_q \sin \alpha)(-\phi_p \sin \alpha + \phi_q \cos \alpha)| \rangle \\ &= \langle |\phi_p \phi_q (\cos^2 \alpha - \sin^2 \alpha) + (\phi_q^2 - \phi_p^2) \sin \alpha \cos \alpha| \rangle \\ &= \langle |\phi_p \phi_q \cos 2\alpha + \frac{1}{2}(\phi_q^2 - \phi_p^2) \sin 2\alpha| \rangle \end{aligned} \quad (10)$$

The result incorporates two terms: the original $\phi_p \phi_q$ product and $(1/2)(\phi_q^2 - \phi_p^2)$. The first term alone would give the spatial overlap $O_{p,q}$ before unitary transformation, and the second term alone would give $O'_{p,q}$ for a $\pm\pi/2$ rotation. In eq 10 the two terms are added with weights depending on α before the modulus is taken, and therefore the result is not simply a weighted sum of the two overlaps.

For a relatively pure p, q transition, that is, a transition without strong involvement of other orbital pairs, the electron density change upon excitation; the difference density $\Delta\rho$ is approximately

$$\Delta\rho \simeq \phi_q^2 - \phi_p^2 \text{ with } \langle \Delta\rho \rangle = 0 \quad (11)$$

Therefore, for an excitation whose transition density is described well by a single occ–vir orbital product, we find for the spatial overlap of the associated auxiliary orbitals of eq 6, that is, for the rotation by $\pm\pi/2$, $O'_{p,q}$ coincides with

$$\frac{1}{2} \langle |\Delta\rho| \rangle \quad (12)$$

Because of conservation of the electron number, the integral of the density change vanishes. However, half the integral over its modulus can serve as a measure of the fraction of an electron that is transferred between spatially disjoint regions. Equation 12 is another, potentially useful, numerical measure of the CT

character of a transition. It can be applied to transitions with more than one dominant MO pair contribution as long as $\Delta\rho$ is calculated explicitly, and it has a straightforward physical interpretation based on the fundamental variable in DFT. Information about the full $\Delta\rho$ is not usually accessible from standard TDDFT linear response calculations, but it can be obtained with additional computational effort within a quadratic response framework or approximated as shown below for the $^1\text{L}_\text{a}$ and $^1\text{L}_\text{b}$ transitions of An and Az.

We note that a large value of $(1/2)\langle|\Delta\rho|\rangle$ may coincide with distance-based criteria for CT, but not necessarily so because the spatially disjoint regions leading to a large value of $(1/2)\langle|\Delta\rho|\rangle$ may be in close proximity, for example, for orbital pairs with compact high-density lobes. Therefore, the density criterion or sizable values of $O'_{p,q}$ may help with the identification of borderline cases that do or do not qualify as CT. In the following, the notation $O'_{p,q}$ indicates a value that is calculated from orbitals, while $(1/2)\langle|\Delta\rho|\rangle$ indicates a value that is calculated from $\Delta\rho$. Further, unless explicitly noted otherwise, $O'_{p,q}$ refers to the orbital combination of eq 6, meaning a two-orbital rotation with an angle of $\pm\pi/2$.

To further illustrate the concept, consider a transition involving a single orbital pair, with $O_{p,q} = \langle|\phi_p\phi_q|\rangle = 0$ such that both orbitals are perfectly spatially separated:

$$\begin{aligned} O'_{p,q} &= \frac{1}{2}\langle|\phi_q^2 - \phi_p^2|\rangle \\ &= \frac{1}{2}\langle|\phi_q^2| + |-\phi_p^2|\rangle \text{ (spatial separation)} \\ &= \frac{1}{2}\langle|\phi_q^2| + |\phi_p^2|\rangle = 1 \end{aligned} \quad (13)$$

The interpretation of O' in terms of the density change as in eq 12 then shows that, upon excitation, a full electron is transferred between spatially disjoint regions. On the other hand, if the two orbitals have complete spatial overlap, $O_{p,q} = 1$, we must have $\phi_q^2 - \phi_p^2 = 0$ everywhere, and consequently $O'_{p,q} = (1/2)\langle|\phi_q^2 - \phi_p^2|\rangle = 0$. In this case, no charge is transferred between regions where the orbitals have no spatial overlap.

Equation 10 incorporates these two extreme situations as special cases. In a clear-cut CT situation, the participating orbitals are spatially disjoint, and the smallest $O'_{p,q}(\alpha)$ will be found for $\alpha = 0$, that is, for the untransformed set of orbitals. However, when the orbitals strongly overlap spatially we have the opposite extreme, and $O'_{p,q} = (1/2)\langle|\phi_q^2 - \phi_p^2|\rangle$ for the $\pm\pi/2$ rotation is small, indicating also a small value of $(1/2)\langle|\Delta\rho|\rangle$ if the approximation in eq 11 holds.

Per this analysis, a criterion for a CT-like transition may therefore rather be an appreciable nonzero value of $O'_{p,q}(\alpha)$ for the $\pm\pi/2$ rotation or—more generally—a sizable $(1/2)\langle|\Delta\rho|\rangle$ integral, as long as the term ‘CT-like’ is supposed to imply that the excitation has characteristics of physical charge transfer. In the interpretation of Kuritz et al. CT-like character is indicated by small $O'_{p,q}$ auxiliary overlaps. It was stated explicitly that CT-like cases such as $^1\text{L}_\text{a}$ transitions of acenes are not CT excitations in the sense of eq 4. This means that CT-like as defined by small $O'_{p,q}$ does not have the characteristics of physical CT and is therefore very unlike CT. We propose that a term such as CT-like should imply the following: (i) A CT-like transition has some of the same physical characteristics as CT but is not clear-cut, implying—among other criteria—borderline small or even rather large spatial overlaps of the orbitals and sizable $(1/2)\langle|\Delta\rho|\rangle$. (ii) Significant improvements from

(tuned) LC functionals versus standard non-hybrid and hybrid functionals are obtained. (iii) Improved excitation energies toward accurate benchmark data (and experiment) when switching to LC functionals are obtained for the right reasons, and they are physically related to the improvements for proper CT.

To provide reference values for a molecule that one may consider too small for supporting a CT or CT-like π to π^* excitation, we calculated the relevant overlaps of H and L for Et. The data are provided in Table 1. We find an expected large

Table 1. Spatial Overlaps, eqs 4 and 9, and Orbital Centroid Distances, eqs 5 and 8^a

	<i>p</i>	<i>q</i>	$O_{p,q}$	$O'_{p,q}$	$\Delta r_{p,q}$	$\Delta r'_{p,q}$
BP	H	L	0.88	0.28	0.06	2.98
	H-1	L	0.62	0.64	1.18	2.07
	H	L+1	0.60	0.66	1.63	1.83
	H	L	0.87	0.28	0.00	1.59
	H-1	L	0.63	0.59	0.00	2.97
	H	L+1	0.65	0.60	0.00	2.92
An	H	L	0.86	0.31	0.11	1.13
	H-1	L	0.69	0.58	1.62	2.78
	H	L+1	0.67	0.59	1.42	2.86
CN9	H	L	0.73	0.50	0.36	4.59
Et	H	L	0.88	0.30	0.00	1.46
DMABN	H	L	0.73	0.56	1.54	2.72
Az	H	L	0.53	0.70	0.88	0.84
	H-1	L	0.84	0.40	0.85	2.49
	H	L+1	0.83	0.40	0.90	2.58
DANS	H	L	0.54	0.75	6.22	3.95
TCNE-B	H	L	0.14	0.98	3.56	0.00

^aKS orbitals from PBE calculations. Isosurface plots of some of the orbitals are shown in Figure 4. A prime indicates that the quantities were calculated for linear combinations of the orbitals according to eq 6. $O_{p,q}/O'_{p,q}$ are dimensionless, $\Delta r_{p,q}/\Delta r'_{p,q}$ are given in Å. $O'_{p,q}$ is for the $\pm\pi/2$ rotation, as in eq 6.

$O_{\text{H,L}} = 0.88$, along with $O'_{\text{H,L}} = 0.30$ similar to the corresponding value for An. The relative performance of TDDFT for Et is good, given the large value of the singlet excitation energy. The LC* result is ~ 0.3 eV below the CCSD(T) benchmark and less than 0.1 eV higher than a standard GGA functional. The corresponding differences for An $^1\text{L}_\text{a}$ (vide infra) are 0.16 and 0.56 eV, respectively, showing substantial CT-like improvements from the tuned LC functional.

3.2. Transformations among Four Orbitals: An Versus Az. The two-by-two orthogonal transformation discussed above can be generalized to include any number of orbitals. Consider An and Az, shown in Figure 1. Both cases afford two singlet π -to- π^* transitions that are usually labeled $^1\text{L}_\text{a}$ and $^1\text{L}_\text{b}$. While the $^1\text{L}_\text{a}$ transition is dominated by the H-L pair, the $^1\text{L}_\text{b}$ transition density is composed of nearly 50/50 weighted pairs of H-1-L and H-L+1 products. From benchmarks in the literature it is known that the $^1\text{L}_\text{a}$ excitation energy is poorly predicted by TDDFT with standard functionals, while the $^1\text{L}_\text{b}$ energy is well-predicted for An, and the opposite was found for Az. To examine these interesting cases the $O'_{p,q}$ criterion suggested by Kuritz et al. is considered for the set of four orbitals involved in the $^1\text{L}_\text{a}$ and $^1\text{L}_\text{b}$ transitions.

In Figure 2, $O'_{p,q}(\alpha)$ is plotted versus the rotation angle α (see eq 7a) for pertinent orbital pairs involved in the

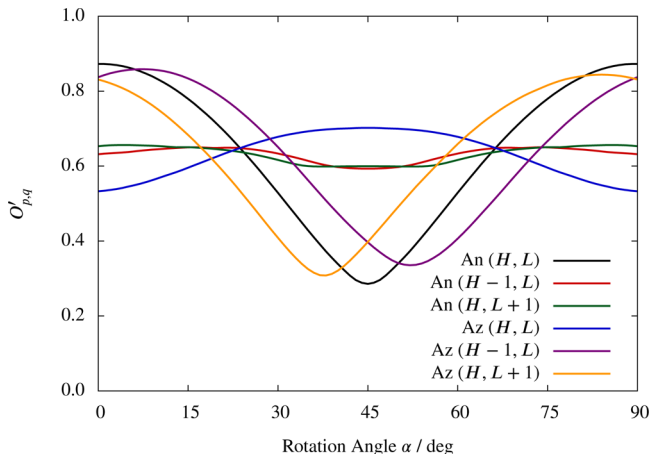


Figure 2. $O'_{p,q}$ as a function of rotation angle for An and Az orbital pairs involved in the L_a and L_b transitions. The orbital pairs are indicated in parentheses.

aforementioned excitations. The An $O'_{H,L}$ curve dips below 0.5. According to the Kuritz et al. criterion, the excitation should be considered CT-like and expected to be relatively poorly predicted by TDDFT. Conversely, the Az $O'_{H,L}$ data do not exhibit this behavior, and the excitation energy should be well-predicted by TDDFT. The orbital products involved in the 1L_b transition display the opposite behavior; that is, the Az $O'_{H-1,L}/O'_{H,L+1}$ curves dip below 0.5, and the An curves do not. Therefore, the Az 1L_b energy should be poorly predicted, and the An 1L_b energy should be well-predicted. These findings appear to be consistent with results from computations. However, as argued by Kuritz et al., if there is any unitary transformation producing small O' overlaps among the orbitals contributing dominantly to an excitation, this should indicate potential CT-like problems. It is, therefore, important to examine unitary transformations among all four orbitals. (The reader is reminded that the Kuritz et al. criterion does not

necessarily mean the same as our working definition of 'CT-like'.)

An antisymmetric 4×4 matrix \mathbf{W} can be formed to produce an orthogonal transformation matrix \mathbf{U} , computed as the matrix exponential of \mathbf{W} . The transformed orbital set is then computed as

$$(\phi'_p, \phi'_q, \phi'_r, \phi'_s) = (\phi_p, \phi_q, \phi_r, \phi_s) \mathbf{U} \quad (14)$$

The prime indicates the transformed orbitals. Using the transformed orbital set we can calculate the auxiliary spatial overlap matrix \mathbf{O}' . For Az and An, the original orbital set includes H-1, H, L, and L+1, and the six overlaps between different orbitals in the original and the transformed set were analyzed. To generate transformed orbitals, the six unique components in \mathbf{W} were varied from 0 to π in increments of $\pi/10$, providing 10^6 representative matrices \mathbf{O}' . A condensed version of the analysis is shown in Figure 3. The percent contribution of a particular orbital pair p,q to an off-diagonal element of \mathbf{O}' is plotted on the abscissa. The ordinate indicates the range of magnitudes of the resulting calculated \mathbf{O}' components. For each element of \mathbf{O}' , and for a particular orbital pair p,q , the plots appeared very similar, and therefore the data for all six off-diagonal elements of \mathbf{O}' were combined in a single graph. The similar appearance of the individual plots (not shown) is reassuring: If all possible parameters in matrix \mathbf{W} were sampled, each individual off-diagonal element of \mathbf{O}' should be representative of all possible pairs of transformed orbitals meaning that the plots for each one should appear identical. A 100% contribution on the abscissa means that the value of the component in \mathbf{O}' was generated from a unitary transformation that only included the orbital pair listed below the abscissa. A 0% value indicates unitary transformations that only included orbitals other than the pair listed below the abscissa. Therefore, for the transformations considered here, the plots for H-1-L and the plots for H-L+1 for a given molecule should be mirror images of each other. This is indeed what Figure 3 shows.

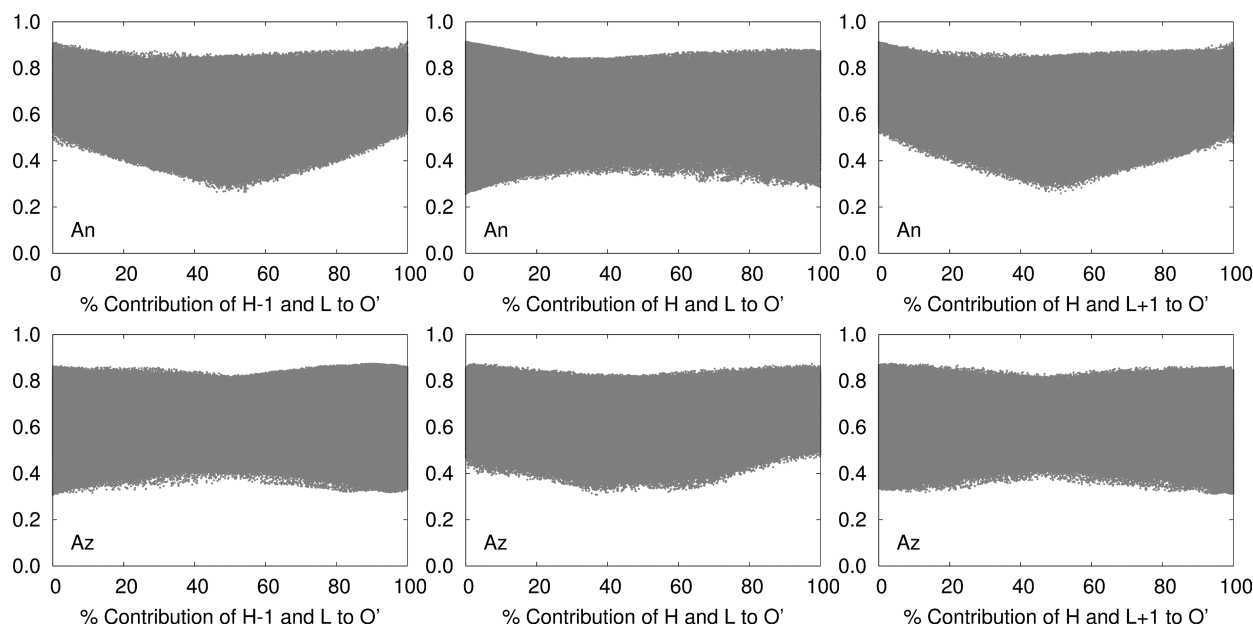


Figure 3. Range (gray) of magnitudes of the off-diagonal elements of \mathbf{O}' for An and Az vs percent contributions of various untransformed orbital pairs to the off-diagonal elements of \mathbf{O}' . PBE orbitals. See text for details.

Table 2. $(1/2)\langle|\Delta\rho|\rangle$ from TDDFT Calculations and Singlet Excitation Energies ΔE from Different Types of Calculations, and Literature Data.^a

		$(1/2)\langle \Delta\rho \rangle$			ΔE						
		PBE	LC*		PBE	B3LYP	LC*	PT2	CCSD	CCSD(T)	lit
		rel	rel	froz							
BP	L_a	0.18	0.24	0.30	3.37	3.68	3.97	4.21	4.39	4.09	$3.96^b, 3.84^c$
	L_b	0.22	0.19	0.23	3.24	3.59	3.78	3.68	3.81	3.50	$3.47^b, 3.40^c$
An	L_a	0.23	0.29	0.29	2.94	3.21	3.50	3.82	4.01	3.66	$3.60^d, 3.69^e$
	L_b	0.14	0.16	0.16	3.64	3.86	3.97	3.86	3.91	3.57	$3.64^d, 3.89^e$
DBAn	L_a	0.32	0.29	0.31	3.09	3.44	3.72	4.15	4.19	3.91	$4.07^b, 3.95^c$
	L_b	0.22	0.20	0.23	3.22	3.60	3.80	3.97	3.86	3.57	$3.41^b, 3.34^c$
CN9		0.20	0.28	0.55	3.47	3.50	3.40	2.80	3.12	2.78	$2.96, 2.81, 2.96^h$
Et		0.32	0.32	0.34	7.80	7.73	7.86	8.09	8.43	8.16	$7.66, \sim 8.0^f, 8.05^g$
DMABN		0.38	0.39	0.56	4.32	4.63	4.80	4.70	5.01	4.72	4.56^k
Az	L_a	0.49	0.55	0.68	2.33	2.40	2.35	2.19	2.31	1.94	$2.13^i, 2.25^j, 2.31^j$
	L_b	0.20	0.23	0.21	3.49	3.63	3.75	3.82	4.02	3.64	$3.99^j, 3.95^j$
DANS		0.67	0.55	0.75	2.16	2.68	3.30	3.60	3.85	3.63	3.32^l
TCNE-B		1.07	1.25	0.98	1.35	1.89	3.13	3.77	3.93	3.69	$3.59^{m\prime}$

^aLC* is short for the IP-tuned LC-PBE* functional. $(1/2)\langle|\Delta\rho|\rangle$ from $\Delta\rho$ obtained from a TDDFT excited-state gradient code (see Section 2). The integrals were generated from cube files similarly to Table 1. “rel” is short for relaxed where the TDDFT calculation used all orbitals. “froz” values were obtained by only allowing the major orbitals to contribute to the TDDFT excitation vectors, i.e., a four-level model for the 1L_b transitions and a two-level model (H and L) otherwise. ^bExperimental data after a correction between $\Delta E(0-0)$ and $\Delta E(\text{vert})$ (0.12 eV for 1L_a and 0.07 for 1L_b) from refs 19 and 67. ^cExperimental data after a solvent correction from refs 18 and 67. ^dExperimental data from ref 19. ^eCC2 calculation from ref 19. ^fGas-phase experiment from ref 68. ^gEOM-CCSD/6-311++G(2d,2p) calculation from ref 69. ^hexCC3, CASPT2, and GW/BSE calculations from refs 70 and 71. ⁱExperimental data from ref 72. ^jCCSDR(3) and CC2 calculations from ref 73. ^kGas-phase experiment from ref 2. ^lRI-CC2 calculation from ref 33. ^mExperimental data from ref 10.

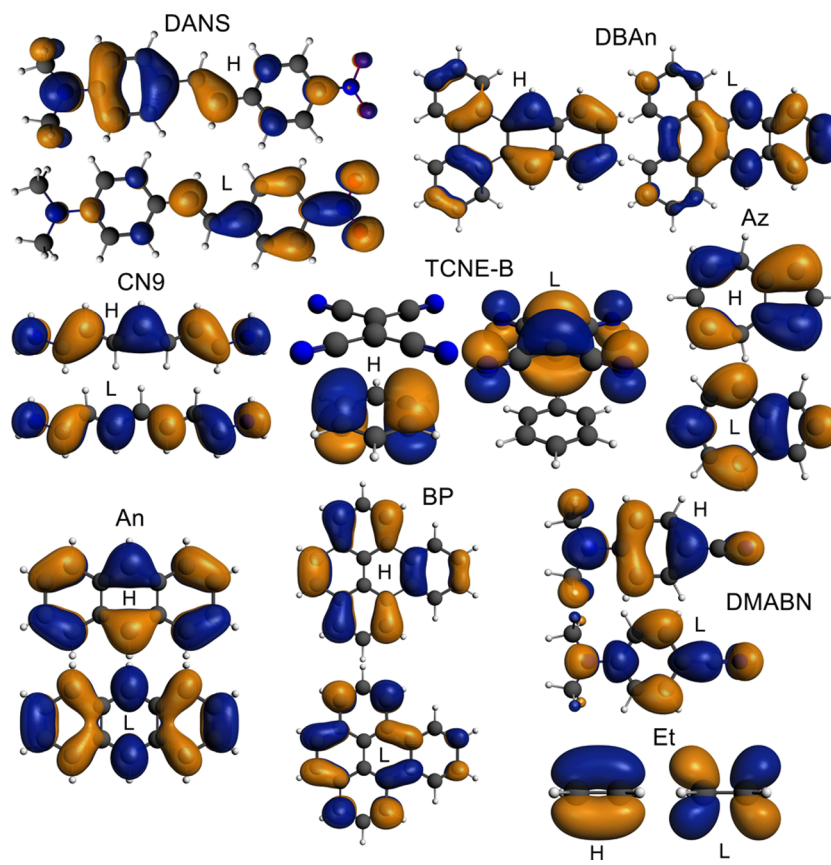


Figure 4. Isosurface plots of selected MOs determined with the PBE functional; isosurface values are 0.03 au. H = HOMO, L = LUMO.

For the 1L_a transition, one is interested in the center plots of Figure 3, which list the H and L contributions to O' , and specifically in the range of overlaps at 100% since the

transitions are of relatively pure H–L character. Indeed, at the 100% contribution, O' for Az does not drop below 0.5, while for An, O' reaches as low as 0.3, which supports the

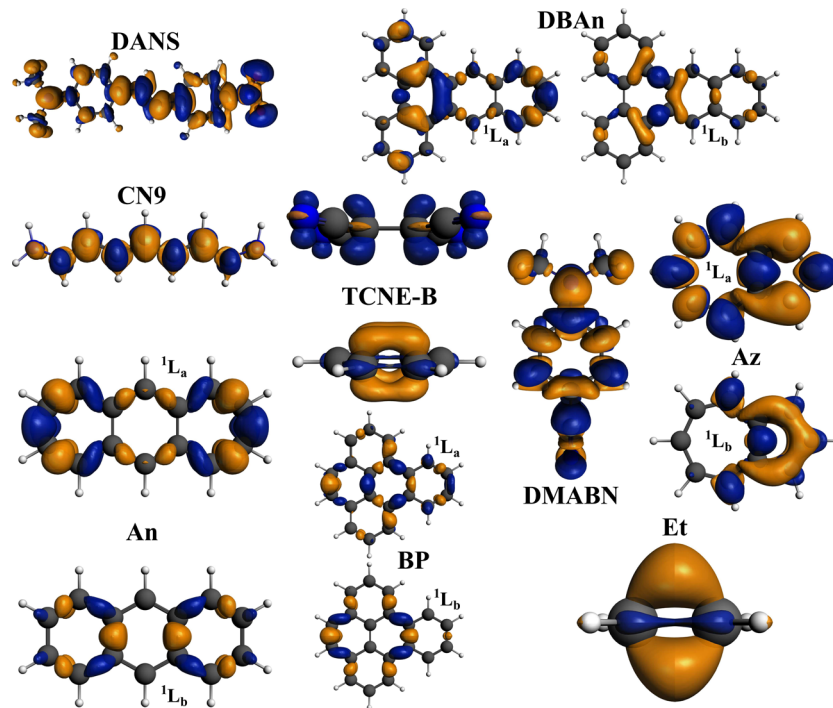


Figure 5. Difference density $\Delta\rho$ for selected excitations, from TDDFT calculations with the PBE functional. Isosurface value is 0.006 au for Et and TCNE-B and 0.001 au for all others. Blue/dark means density gain, orange/light means density loss. Figures S10 and S11 in the Supporting Information display the corresponding density changes from TDDFT/LC* and CASPT2.

Kuritz et al. analysis. The latter value is for the $\alpha = \pm\pi/2$ rotation of the H–L pair and therefore indicates an approximate value of $(1/2)\langle|\Delta\rho|\rangle$ similarly small as for Et, as already noted, meaning that the excitation affords little physical CT. For Az, on the other hand, the $\alpha = \pm\pi/2$ rotation of the H–L pair gives $O' = 0.70$. When this value is considered as an approximation for $(1/2)\langle|\Delta\rho|\rangle$ it indicates a significant density shift among spatially disjoint regions upon excitation. Nonetheless, TDDFT with standard functionals appears to perform well for the $^1\text{L}_a$ excitation of Az. We show below that this can be viewed as an error compensation.

The $^1\text{L}_b$ transition is assigned to an ~50/50 weighted combination of H–1–L and H–L+1 orbital pairs. To reiterate, it is considered to be well-predicted for An with TDDFT and conventional functionals but poorly predicted for Az. Here, all of the graphs in Figure 3 are of relevance. For both molecules there are regions in the plots where O' values drop to 0.3 or even below. According to the criterion by Kuritz et al. the presence of such small auxiliary spatial overlaps would indicate a CT-like situation for both molecules, and consequently for both molecules TDDFT with standard functionals should perform poorly for $^1\text{L}_b$, contrary to what has been noted in the literature. An alternative scheme of transforming the orbitals is discussed in the Supporting Information, which excludes certain cases of the 4×4 transformation to avoid generating O'_{pq} values where both ϕ'_p and ϕ'_q lie only in the occupied or only in the virtual space. Figure S18 shows that also in this case the ranges of spatial overlaps are as large as in Figure 3.

Full calculations of $(1/2)\langle|\Delta\rho|\rangle$ for these and the other molecules are discussed in Section 3.3 and show that these integrals are small for the $^1\text{L}_b$ excitations and do not indicate much physical CT. Assuming that the excited-state versus ground-state density has a similar weight of H–1–L and H–L+1 contributions as the TDDFT transition density, which is

about 50/50, the difference density for the $^1\text{L}_b$ excitation can be approximated as

$$\Delta\rho \approx \frac{1}{2}[\phi_{\text{L}+1}^2 + \phi_{\text{L}}^2 - \phi_{\text{H}}^2 - \phi_{\text{H}-1}^2] \quad (15)$$

Numerical evaluation of $(1/2)\langle|\Delta\rho|\rangle$ from eq 15 with ground-state PBE orbitals gives only 0.15 for An (see Supporting Information, Table S9), in excellent agreement with a four-level TDDFT value for $(1/2)\langle|\Delta\rho|\rangle$ for the PBE functional in Table 2, indicating significantly less CT character for the An $^1\text{L}_b$ transition compared to $^1\text{L}_a$. For Az, the values for both transitions are higher, but the density criterion also assigns more character of CT to $^1\text{L}_a$ than to $^1\text{L}_b$. The validity of the simple model for the $^1\text{L}_b$ density change in eq 15 and the corresponding value generated from the TDDFT calculations has further been confirmed by a CAS(4,4) calculation for An. The second excited state has 49% weight from the H to L+1 excited configuration and 50% weight from the H–1 to L excited configuration, with occupations of the active natural orbitals of 1.48, 1.50, 0.52, and 0.50, respectively. The integrals of $(1/2)\langle|\Delta\rho|\rangle$ for the $^1\text{L}_a$ and $^1\text{L}_b$ CASSCF excited states are 0.29 and 0.16, in agreement with the DFT-based data. The corresponding plots of the density change are shown in Figure 5 and in the Supporting Information in Figures S10 and S11.

In the light of the meaning of O' for a symmetric molecule and a transition dominated by one orbital pair to represent an approximation of $(1/2)\langle|\Delta\rho|\rangle$, and considering the ambiguous findings for the $^1\text{L}_a$ and $^1\text{L}_b$ transitions of An versus Az for the auxiliary overlaps and the density criterion versus TDDFT performance, it is unclear whether the spatial overlap among arbitrary orthogonal transformations of sets of MOs can reliably indicate a CT-like situation. A more pragmatic working definition for a CT-like case may be whether an excitation energy is improved by using tuned LC functionals similar to

clear-cut CT cases. The question then remains what the actual problem with CT-like situations and standard functionals really is. We aim to answer this question in the following subsections.

3.3. Charge Transfer Character Based on Overlaps, Distances, and $\Delta\rho$, Versus TDDFT Performance. We now turn to the full set of molecules of Figure 1 and examine various numerical criteria by which the extent of CT character of the excitations may be assessed. The accuracy of the excitation energies for different types of functionals in TDDFT is also examined by comparison with correlated wave function calculations and relevant literature data. CCSD and CCSD(T) data are used to assess the quality of the excitation energies. Some data related to the excitations are collected in Tables 1 and 2. The ordering of the molecules in the Tables, here and in the Supporting Information, is by increasing $(1/2)\langle|\Delta\rho|\rangle$ as determined with the LC* functional. Isosurfaces of selected MOs for the various molecules are shown in Figure 4. The CT criteria discussed in Section 3.1 are examined first, followed by an examination of various integrals that enter the TDDFT excitation energies and may indicate CT and CT-like situations.

Up-front, it is important to note that in all cases the CCSD(T) excitation energies are significantly below those from CCSD, by several tenths of an electronvolt in most cases. We also performed calculations with the CC2 approximation to CCSD (see Supporting Information, Table S8) and found in some cases several tenths of an electronvolt differences with respect to CCSD, indicating important electron correlation effects. In light of the substantial corrections from the perturbative triples in the CC calculations, previous assessments of the performance of TDDFT based on comparisons with CC2 and methods of similar accuracy may need to be reconsidered. For instance, the nearly 0.4 eV drop of the $\text{Az}^{\text{1}}\text{L}_b$ energy when going from CCSD to CCSD(T) brings it in reasonable agreement with all density functional results. The $\text{An}^{\text{1}}\text{L}_a$ excitation remains a challenge for PBE and B3LYP. By comparison with CCSD, LC* appears to perform very well for $\text{An}^{\text{1}}\text{L}_b$. However, with respect to the CCSD(T) benchmark all functionals overestimate the $\text{An}^{\text{1}}\text{L}_b$ energy, and significantly so with LC*.

To set a “baseline” regarding the CT criteria, compare Et with the CT complex TCNE-B. The lowest-energy π -to- π^* singlet excitation of Et involves a compact set of valence orbitals that, due to the small size of the molecule and the compact nature of the involved orbitals, cannot reasonably be labeled CT or CT-like. Indeed, the H–L spatial overlap is large, $O_{\text{H,L}} = 0.88$. The auxiliary overlap $O'_{\text{H,L}} = 0.30$ —indicating also the approximate value of $(1/2)\langle|\Delta\rho|\rangle$ —is not very large. The actual $(1/2)\langle|\Delta\rho|\rangle$ value from TDDFT is 0.32 (Table 2, LC*), in excellent agreement with the estimate from the H–L pair, showing that relaxation contributions to the excited-state density from other orbitals are small. Because of the symmetry of the molecule, the centroid criterion $\Delta r_{\text{H,L}}$ is zero. For the transformed orbital pair, $\Delta r'_{\text{H,L}} = 1.46$ is large given the small size of Et, which goes along with the relatively small value of $O'_{\text{H,L}}$. In terms of relative accuracy, TDDFT is reasonably close to the literature values of 8.0 to 8.05 eV for the vertical excitation energy, to the CC data, and the 8.09 eV from our CASPT2 calculation. The TDDFT results are much below the CCSD energy, but CCSD(T) gives a correction of −0.3 eV. While CT is not an issue here, the transition involves compact orbitals and is therefore sensitive to the level at which correlation is treated.

TCNE-B, previously studied by Stein et al.¹⁰ and other groups, is a clear-cut CT case: The H–L spatial overlap $O_{\text{H,L}} = 0.14$ is very small, and for the transformed orbital pair $O'_{\text{H,L}} = 0.98 \approx (1/2)\langle|\Delta\rho|\rangle$ (PBE) = 1.07 indicates the transfer of a full electron from benzene to TCNE upon excitation. The orbital centroid distances are in line with the spatial overlap data and the $\Delta\rho$ criterion, being 3.56 Å for the H–L pair and zero for the transformed pair. Note that TCNE and benzene are at a distance of ∼3.6 Å in the complex. Therefore, for this essentially complete charge transfer between small subsystems the $\Delta r_{\text{H,L}}$ criterion measures the spatial range of the CT accurately. We note that the relaxed $(1/2)\langle|\Delta\rho|\rangle$ from the TDDFT/LC* calculation is significantly above 1, meaning that along with the CT the value additionally measures orbital reorganization within the donor and acceptor moieties. As expected for this CT complex, the performance of TDDFT with conventional functionals is extremely poor, underestimating the excitation energy ΔE by more than 2 eV with PBE. The LC* functional performs much better but remains somewhat below experiment and the CCSD(T) benchmark.

A less-than-complete CT case is represented by DANS, a π -conjugated donor–acceptor (“push–pull”) chromophore with an intense low-energy singlet π - π^* excitation. We have recently studied the nonlinear optical (NLO) response of this and related systems with IP-tuned RS functionals³³ and found the tuning procedure to improve the CT excitation energies and NLO response dramatically. The data in Tables 1 and 2 show $O'_{\text{H,L}}$ close to 0.8 and $(1/2)\langle|\Delta\rho|\rangle$ (PBE) close to 0.7. This indicates a strong CT character for the transition, with more than half of an electron being transferred among spatially disjoint regions upon excitation. The spatial overlap $O_{\text{H,L}}$ between H centered at the donor and L centered at the acceptor moiety is roughly 0.5, which is not very small because both orbitals are delocalized over the π -bridge.³³ The very large value of $\Delta r_{\text{H,L}} = 6.22$ appears to indicate an even more pronounced CT character than for TCNE-B. The fact that $\Delta r'_{\text{H,L}} = 3.95$ for the transformed orbital pair is also quite large, however, indicates that the CT is not complete because the orbitals overlap over a range of ∼2 Å due to their mutual strong delocalization over the π bridge. The comparison of $O_{\text{H,L}}$ with $O'_{\text{H,L}}$, the distance criteria, as well as the magnitude of $(1/2)\langle|\Delta\rho|\rangle$, all indicate that the DANS excitation has a strong but incomplete CT character. The incomplete CT for DANS is reflected in the performance of TDDFT. While CCSD(T) and experimental data for the singlet excitation energies of TCNE-B and DANS are similar, between 3.3 and 3.6 eV, the underestimation of this energy by PBE is less pronounced for DANS, albeit still unacceptable. LC* is in excellent agreement with CASPT2 and experiment, but 0.3 eV below the CCSD(T) benchmark. The relaxed $(1/2)\langle|\Delta\rho|\rangle$ (LC*) value of 0.55 in this calculation is significantly below the two-level model LC* (0.75); that is, there is pronounced orbital relaxation upon excitation.

Another well-known π -conjugated donor–acceptor molecule is DMABN.² This molecule has attracted interest due to its dual fluorescence.⁷⁴ The anomalous emission in DMABN is related to an intramolecular CT state assigned to the H–L pair. In contrast with DANS, conventional functionals provide a reasonable CT excitation energy for DMABN, although PBE is still 0.4 eV too low. The centroid distance $\Delta r_{\text{H,L}}$ for the orbitals of DMABN involved in the excitation is 1.54 Å. According to the centroid criterion put forward by Guido et al.,⁴ a Δr shorter than ∼1.5 Å indicates a short-range (SR)

excitation where traditional GGA and hybrid functionals should perform reasonably well, while range-separated functionals provide no particular benefit. In line with these findings, the spatial overlap of H and L is comparatively large (0.73), although the overlap of the transformed orbitals indicates that about half of an electron is transferred between spatially disjoint regions upon excitation. The system may therefore be classified as having SR CT. The full TDDFT $\langle 1/2 \rangle \langle |\Delta\rho| \rangle$ value is smaller than $O'_{H,L}$, just below 0.4, due to contributions to $\Delta\rho$ from other orbital pairs. The tuned functional LC* slightly overestimates the energy of this excitation.

Another interesting situation is represented by cyanine dyes. A member of the cyanine family with nine atoms in the conjugated backbone (CN9, shown in Figure 1). Many groups have investigated the unintuitive performance of TDDFT for the first excitation energies of the cyanine dyes,^{70,75–81} including recent studies by our group,³⁴ Ziegler and collaborators,⁸² and Jacquemin et al.⁷¹ Unlike for many other chromophores, TDDFT with standard functionals systematically overestimates the energies of the cyanine H–L transitions. Semilocal functionals such as PBE give closer agreement with experiment, while global hybrid functionals such as B3LYP and PBE0 perform particularly poorly. Moreover, IP-tuned RS functionals give hardly any improvements over global hybrids for the cyanines, ruling out severe problems due to the DFT delocalization error and the CT issue. The analysis in ref 34 and others pointed to differential correlation between the ground and excited state for the singlet excitation that is poorly described by DFT, rather than a CT-like character of the transition. At the same time, the analogous triplet excitation is underestimated in energy by DFT. For CN9, $O'_{H,L} = 0.73$ with the PBE functional. However, $O'_{H,L} = 0.50$ is much larger than the corresponding value for An and more similar to DMABN. As it was pointed out previously,⁸³ there is a large density shift in the cyanine backbone and bonds between them, upon excitation. We previously did not interpret the $O'_{H,L}$ value as indicating a CT-like situation because of the proposed criterion of small $O'_{H,L}$ from ref 3. However, its interpretation as an approximation for $\langle 1/2 \rangle \langle |\Delta\rho| \rangle$ adds a slight twist to the cyanine story that may give a clearer picture. On the basis of the large $O'_{H,L}$ value, it appears appropriate to attribute an SR CT character to the excitations, similar to DMABN. This would rationalize the too-low triplet excitation energies for semilocal functionals and global hybrids with small fractions of exact exchange. Since the shift of electron density upon excitation is short-ranged, the use of long-range eX in an RS functional is of no help. The reason for the overestimation of the singlet excitation energy is connected to a large H–L exchange ERI, as discussed in Section 3.4.

Another point worth noticing is that, while $O'_{H,L}$ for the cyanine is large, the full $\langle 1/2 \rangle \langle |\Delta\rho| \rangle$ is only 0.20 (PBE) to 0.28 (LC*). This indicates that orbital reorganization is rather pronounced in the excited-state density.

For the $^1\text{L}_a$ excitation of Az, the large $O'_{H,L} = 0.70$ indicates a significant shift of electronic charge. The LC* two-level TDDFT value is close, while the fully relaxed TDDFT values of $\langle 1/2 \rangle \langle |\Delta\rho| \rangle$ are in the range from 0.5 to 0.6. (~0.6 for CAS(4,4)). Considering the short centroid distance of 0.88 Å and an intermediate spatial overlap $O_{H,L} = 0.53$, the situation appears to be somewhat similar to DMABN and the cyanine, in particular, when considering the low CCSD(T) excitation energy. That is, whereas the previous analysis of $O'_{H,L}$ appeared to indicate that the good agreement of TDDFT with CC2 and

similarly performing methods was for the right reasons, the present results indicate SR CT character with a cyanine-like overestimation of the excitation energy by TDDFT.

The calculated $\langle 1/2 \rangle \langle |\Delta\rho| \rangle$ for the $^1\text{L}_b$ transition of Az is 0.20 for PBE and 0.23 for LC*, and it is similar in the two-level model. The small density shift and lack of much relaxation through involvement of other orbitals should mean that the $^1\text{L}_b$ excitation energy is reasonably predicted by TDDFT with standard functionals. Given that our new CCSD(T) benchmark is a full 0.4 eV below the corresponding CCSD value, it turns out that the performance of TDDFT is indeed good, with B3LYP being spot-on.

Benzo[*e*] pyrene (BP) and dibenz[*a,c*] anthracene (DBAn) have been studied previously by Richard and Herbert.¹⁸ The two nonlinear polycyclic aromatic hydrocarbon (PAH) molecules are isomers of pentacene. For BP, PBE severely underestimates the $^1\text{L}_a$ excitation energy, which improves a lot with B3LYP and in particular with LC*. For $^1\text{L}_b$, the situation is less clear-cut, with PBE too low and LC* too high—but the trend from low to high is the same. For DBAn the situation is similar, with $^1\text{L}_a$ severely underestimated by PBE and improved a lot with LC*. The trend for $^1\text{L}_b$ is also the same as for BP, with increasing energy from PBE to LC*, bracketing the CCSD(T) benchmark. In both cases, the $^1\text{L}_b$ energies from LC* are close to CCSD, but the triples corrections are ca. –0.3 eV, and the PBE energies are too low but not severely so. Richard and Herbert found it essentially impossible to provide a useful diagnostic tool discerning any CT character based on the MOs, difference density plots, natural transition orbitals, or transition densities and excited-state atomic charges. According to the criterion by Kuritz et al., the $O'_{H,L}$ values are small for both molecules (0.28 and 0.31, BP and DBAn, respectively) and therefore may indicate a CT-like situation in each case. The calculated $\langle 1/2 \rangle \langle |\Delta\rho| \rangle$ values for the $^1\text{L}_a$ and $^1\text{L}_b$ states are roughly 0.2–0.3 BP and DBAn, respectively, indicating no pronounced physical CT.

To summarize this subsection, singlet excitations that are obvious CT cases based on the criteria of small spatial overlap and large centroid distances are very strongly underestimated by conventional TDDFT functionals. In this case the $\langle 1/2 \rangle \langle |\Delta\rho| \rangle$ criterion then also indicates the transfer of a substantial fraction of an electron between spatially disjoint regions. However, there remains a challenge for CT-like situations with PAH molecules such as the examples shown in Figure 1, push–pull chromophores with short π bridges, or the cyanine chromophore. Conventional TDDFT calculations sometimes poorly predict π -to- π^* singlet excitation energies for states that do not indicate significant CT character based on the spatial overlaps $O_{p,q}$, the centroid distances $\Delta r_{p,q}$, or $\langle 1/2 \rangle \langle |\Delta\rho| \rangle$ values. At the same time, small $O'_{p,q}$ values are not reliable indicators of a CT-like situation as evidenced by the comparison of the transitions for An and Az in Section 3.2. When considering that for a transition dominated by a single orbital pair the $O'_{p,q}$ overlap is a good approximation for $\langle 1/2 \rangle \langle |\Delta\rho| \rangle$, the data for BP and DBAn also do not reveal CT-like situations. We show in the following subsection that the poor performance of TDDFT with standard non-hybrid functionals and global hybrids for CT-like singlet excitations is unlikely to be associated with the CT problem.

3.4. Other Numerical Measures for the Charge-Transfer Character and for Diagnosing TDDFT Problems. Two-Level Models for Analyzing the Excitation Energies. It has been known for a long time^{1,16,84,85} that

DFT-based ΔSCF with approximate functionals sometimes gives accurate excitation energies in cases where LR TDDFT with semilocal or global hybrid XC response kernels produce large errors. ΔSCF refers here to calculations using the difference between the ground-state Kohn–Sham (KS) energy and the energy of a KS determinant representing an excited configuration, with the energy being minimized self-consistently with respect to the orbitals in each case. We use the notation ΔD to indicate KS energy differences with (frozen) ground-state orbitals used in both KS determinants. Casida et al.¹ have previously analyzed problems with TDDFT LR excitation energy calculations by comparing the expressions for the excitation energies for a linearized TDDFT versus a ΔD two-level model. We have subsequently used such comparisons to analyze other difficult cases for TDDFT such as the aforementioned cyanine chromophores³⁴ and ligand-field transitions of 3d metal complexes¹⁶ and found the equations to provide insight into the nature of the problems encountered with TDDFT.

Consider an excitation that only involves a single occupied (*i*)–virtual (*a*) orbital pair such as H and L. (We use indices *i,a* as in eq 3 as we are not considering transformations as in eq 6, (7a) between occ and vir orbitals.) The linearized TDDFT singlet and triplet excitation energies for such a two-level model are

$$^1\Delta E^{\text{TD}} = (\varepsilon_a - \varepsilon_i) + [a|f_{\text{XC}}^{\alpha\alpha} + f_{\text{XC}}^{\alpha\beta}|lai] + 2[a|r_{12}^{-1}|lai] \quad (16a)$$

$$^3\Delta E^{\text{TD}} = (\varepsilon_a - \varepsilon_i) + [a|f_{\text{XC}}^{\alpha\alpha} - f_{\text{XC}}^{\alpha\beta}|lai] \quad (16b)$$

Here, $f_{\text{XC}}^{\sigma\tau}(1,2)$ is the XC response kernel, σ and $\tau \in \{\alpha, \beta\}$ are orbital spin indices, ε_a and ε_i are ground-state orbital energies, “1” and “2” indicate the spatial coordinates of a pair of electrons, and we assume that the calculation is (as usual) based on the adiabatic approximation such that $f_{\text{XC}}^{\sigma\tau}$ is not frequency-dependent. For a semilocal response kernel, $f_{\text{XC}}^{\sigma\tau}(1,2) = f_{\text{XC}}^{\sigma\tau}(r_1)\delta(r_2 - r_1)$. The shorthand notation for the f_{XC} integrals and the ERIs implies the ordering of electron coordinates and orbitals as in $[p(1)q^*(1) \text{ loperator} | r(2)s^*(2)]$. Assuming a semilocal XC kernel, we have $[a|f_{\text{XC}}^{\sigma\tau}|lai] = [a|f_{\text{XC}}^{\sigma\tau}|li]$.

The expressions for the singlet and triplet excitation energies obtained from ΔD for the two-level model, using $\phi_a^2 - \phi_i^2 = \Delta\rho$ as the density change for the excitation within this model, read

$$^1\Delta E^{\Delta D} = (\varepsilon_a - \varepsilon_i) + \frac{1}{2}[\Delta\rho|r_{12}^{-1} + f_{\text{XC}}^{\alpha\alpha}|\Delta\rho] \\ - [i|f_{\text{XC}}^{\alpha\alpha} - f_{\text{XC}}^{\alpha\beta}|laa] \quad (17a)$$

$$^3\Delta E^{\Delta D} = (\varepsilon_a - \varepsilon_i) + \frac{1}{2}[\Delta\rho|r_{12}^{-1} + f_{\text{XC}}^{\alpha\alpha}|\Delta\rho] \\ + [i|f_{\text{XC}}^{\alpha\alpha} - f_{\text{XC}}^{\alpha\beta}|laa] \quad (17b)$$

after expansion of $E_{\text{XC}}[\rho^\alpha + \Delta\rho^\alpha; \rho^\beta + \Delta\rho^\beta] - E_{\text{XC}}[\rho^\alpha; \rho^\beta]$ in terms of $\Delta\rho^\sigma$ and neglecting terms of higher order. Figure S7 in the Supporting Information demonstrates that the linearized results are very close to the full energy differences for the KS determinants with frozen orbitals.

Casida et al. pointed out¹ that the term $\Delta_{\text{CT}} = (1/2)[\Delta\rho|r_{12}^{-1} + f_{\text{XC}}^{\alpha\alpha}|\Delta\rho]$ on the right-hand side of eqs (17a,b), dubbed the CT term, is an artifact of approximations in DFT. With the exact XC functional, the expressions for the linearized TDDFT

and linearized ΔD two-level excitation energy should become equal. We previously found that the magnitude of Δ_{CT} relative to the excitation energy, or alternatively the orbital energy gap as a crude approximation of the excitation energy, may indicate shortcomings in TDDFT calculations that are otherwise difficult to diagnose.¹⁶

Many of the problems encountered in TDDFT excitation energy calculations can be traced back to the various terms in these expressions. In a linearized time-dependent Hartree–Fock (TDHF) two-level model, $[a|f_{\text{XC}}^{\alpha\alpha} \pm f_{\text{XC}}^{\alpha\beta}|lai]$ of eq 16a is replaced by $-[a|r_{12}^{-1}|li]$, and all terms are evaluated with HF, rather than KS, orbitals. The latter term in TDHF is responsible for the physically correct $-1/R$ behavior of the energy of a CT excitation as a function of the separation R between ϕ_a and ϕ_i . In TDDFT, if the two orbitals are spatially separated and the XC response kernel is semilocal, $[a|f_{\text{XC}}^{\alpha\alpha} \pm f_{\text{XC}}^{\alpha\beta}|lai]$ goes to zero exponentially with the orbital separation, rather than with power -1 , which causes inaccuracies.

The leading term in the excitation energy, $\Delta\varepsilon = \varepsilon_a - \varepsilon_i$, is formally the same in TDDFT and TDHF. However, the numerical value of $\Delta\varepsilon$ is strongly dependent on the chosen functional and in particular on the fraction of exact exchange in hybrid functionals. In HF, $\Delta\varepsilon$ approximates IP – EA, the fundamental gap. For CT excitations, it is desired to have such a leading term in the excitation energy. LC functionals that are tuned as described in Section 2 often produce $\varepsilon_H = -\text{IP}$ and $\varepsilon_L = -\text{EA}$ to an excellent degree. Moreover, for long-range CT with spatially well-separated orbitals the exchange component of $[a|f_{\text{XC}}^{\alpha\alpha} \pm f_{\text{XC}}^{\alpha\beta}|lai]$ effectively switches to the corresponding eX term $-[a|r_{12}^{-1}|li]$ due to the range-separation, providing the $-1/R$ dependence of the CT excitation energy. The correlation component of $[a|f_{\text{XC}}^{\alpha\alpha} \pm f_{\text{XC}}^{\alpha\beta}|lai]$ still vanishes exponentially with orbital separation within functionals where the range-separation is only in the exchange. In an intermediate situation with comparatively large $\phi_a - \phi_i$ overlap—but already in the regime of exponential drop-off—there is then potentially a problem with the HF-like term $-[a|r_{12}^{-1}|li]$ not having a sufficiently large correlation counterpart if the integral is large.

With semilocal functionals, $\Delta\varepsilon$ is usually much smaller than the fundamental gap and often also significantly smaller than the optical gap. While this is not, per se, a problem, the integrals $[a|f_{\text{XC}}^{\sigma\tau}|lai]$ may become too small too quickly if the orbitals separate spatially. The calculated excitation energies are then dominated by the values of $\Delta\varepsilon$ and often end up being too low with semilocal functionals. The excitation energies may then also become strongly functional dependent because $\Delta\varepsilon$ is strongly functional dependent (for this reason, $\Delta\varepsilon$ may be fortuitously close to an excitation energy depending on the choice of functional³⁰).

In eqs (16), the singlet/triplet (S/T) excitation energy difference is given by $2[a|r_{12}^{-1}|lai] + 2[a|f_{\text{XC}}^{\alpha\beta}|lai]$. In TDHF LR theory, the S/T separation is $2[a|r_{12}^{-1}|lai]$ evaluated with the HF orbitals. Correlation effects on the S/T separation show up in two ways: (i) $[a|r_{12}^{-1}|lai]$ being evaluated with the KS, instead of the HF, orbitals, and (ii) via the $[a|f_{\text{XC}}^{\alpha\beta}|lai]$ contributions. The occurrence of two times the exchange ERI in the singlet excitation has its origin in the Coulomb part of the effective molecular potential (hence, it shows up both in TDDFT and in TDHF), whereas the terms involving $f_{\text{XC}}^{\sigma\tau}$ of course originate from the XC potential. In our recent cyanine study,³⁴ numerical data indicated that with semilocal functionals such as PBE the integrals $[a|f_{\text{XC}}^{\alpha\alpha} \pm f_{\text{XC}}^{\alpha\beta}|lai]$ for the H–L pair were rather small and potentially too small in magnitude overall.

For the present work we decided to investigate the magnitude of the various integrals in eqs (16) and (17) and the Δ_{CT} term for the whole set of molecules to learn about their trends when going from no-CT to full-CT across a spectrum that may include CT-like cases. CCSD and CCSD(T) data for the triplet excitation energies were also generated as benchmarks. It should be reiterated that relaxation from orbital pairs other than the ones mainly assigned to the transition can strongly influence the excitation energy, but consideration of such relaxation would render the analysis very cumbersome. We therefore focus on the leading terms derived from the two-level model. The relevant integrals in eqs (16) and (17) for the H–L orbital pairs and, for selected cases, the H–1–L and H–L+1 pairs, are based on PBE KS orbitals and were calculated as described in Section 2. All values quoted in the text are in electronvolts. Integrals over f_{XC} were calculated with an LDA response kernel. Additionally, we performed TDDFT singlet and triplet excitation energy calculations with NWChem with the full PBE response kernel but allowing only H and L to contribute to the LR density matrix. This effectively enforces a two-level model. The results are in excellent agreement with the excitation energies obtained from the integrals explicitly via eqs (16), showing that the density gradient terms in the PBE linear response kernel contribute little to the f_{XC} integrals for our samples. The full set of numerical data can be found in the Supporting Information. A subset of the data is discussed in the following subsections.

The Charge Transfer Term Δ_{CT} . The values of Δ_{CT} for the H–L transitions of the molecule set are shown in Figure 6

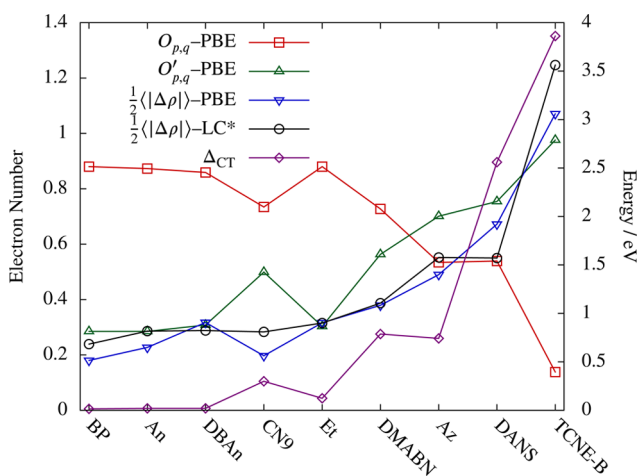


Figure 6. Various CT diagnosis terms, presented in the literature are plotted using the data from Supporting Information, Table S1. δ_{ct} is given in electronvolts units, all other terms are in electron number.

along with other CT diagnostics discussed above. The CT term exhibits a very pronounced trend that roughly follows those of $O'_{p,q}$ and the values of $(1/2)\langle|\Delta\rho|\rangle$. The increase of the latter two criteria roughly mirror the decrease of the spatial H–L overlap $O_{p,q}$. Despite cautious statements in ref 1 that the CT term may not be directly related to actual CT, its largest values, for TCNE-B and DANS, clearly reflect the CT character of the excitations for these systems, and the small values for the PAHs and Et reflect that lack of CT character in their $\pi-\pi^*$ transitions according to other suitable criteria.

The ERIs are the main contributors to Δ_{CT} , but even the negative f_{XC}^{aa} component increases strongly in magnitude across

the molecule set, from –0.04 for BP to –0.57 for TCNE-B. However, except for a few cases (most notably Et, due to its compact orbitals) all f_{XC} integrals are much smaller—below 0.5 eV in magnitude—than most of the ERIs involving the frontier orbitals. In particular, the $[ailf_{XC}^{aa}|ai]$ integrals where the two orbitals differ are small. The corresponding $[ailf_{XC}^{ab}|ai]$ integrals are even smaller and therefore in most cases practically negligible at the accuracy level attainable with TDDFT or CCSD calculations. (The comparatively large value of $[ailf_{XC}^{aa}|ai] = [aaf_{XC}^{ab}|ii] = -0.98$ for the H–L pair of Et must be attributed to the compactness and large spatial overlap of the orbitals.)

The $[ailf_{XC}^{aa}|ai]$ Integrals. The integral $[ailf_{XC}^{aa}|ai]$ becomes very small for the proper CT cases, –0.06 and –0.01 for DANS and TCNE-B, which is expected because of the small spatial overlap between H and L for these molecules. For the other systems, this integral ranges between –0.21 and –0.25 eV with the exception of Az (–0.11), which, however, has a value of $O_{H,L}$ that is almost as small as that for DANS. It appears that in the series An, Az, DANS, TCNE-B an exponential decrease of magnitude of f_{XC} integrals with orbital separation becomes evident. For systems where $O_{H,L}$ is 0.73 or higher these integrals are very similar, on the order of –1/4 eV (with the already noted exception of Et). There is no obvious relation of the magnitude of these integrals and the TDDFT performance other than that with increasing CT character $[ailf_{XC}^{aa}|ai]$ decays too fast and cannot describe the $-1/R$ component in long-range CT energies, as already mentioned. However, as in our previous analysis³⁴ of CN9, the $[ailf_{XC}^{aa}|ai]$ are overall small, potentially rendering the XC corrections to $\Delta\epsilon$ and $2[ailr_{12}^{-1}|ai]$ needed for accurate predictions of excitation energies too small. As pointed out above, however, there can also be an error compensation for singlet excitations if $2[ailr_{12}^{-1}|ai]$ is large and $\Delta\epsilon$ is below the triplet excitation energy. Very small $[ailf_{XC}^{ab}|ai]$ integrals, in particular, indicate a lack of XC contributions to the S/T gap in TDDFT. Good or bad performance of TDDFT for CT-like or non-CT situations may well be influenced by the presence of lack of such error compensation in a way that obscures the distinction of a CT-like problem from an unproblematic case.

Triplet Energies and S/T Separations. Relevant data are collected in Table 3. We assume that the CCSD(T) triplet energies represent a reasonably accurate benchmark and that the TDDFT triplet excitation energies are not adversely impacted by near triplet instabilities (this may be more of an issue with the LC* calculations). The CCSD(T) triplet energies are below the first excited singlet state except for the Az 1L_a transition where the singlet excitation is lower by 0.2 eV. For TCNE-B, the singlet and triplet excitations have nearly the same energy, due to the very small exchange ERI of 0.02 eV caused by the near-complete spatial separation of the donor and acceptor MOs.

We find across the molecule set that the TDDFT calculations underestimate the triplet excitation energies ${}^3\Delta E$, in some cases severely so, with the exception of Az L_b with PBE. For TCNE-B and, to a somewhat lesser degree, DANS, the PBE functional gives a near-complete CT breakdown, with ${}^3\Delta E$ not much different from the small $\Delta\epsilon$ values. LC* is more consistent in the underestimation of ${}^3\Delta E$ across the board. For cases with large spatial overlap of the orbitals, small $(1/2)\langle|\Delta\rho|\rangle$, small Δ_{CT} , that is, weak to no CT, the PBE and LC* triplet energies are quite similar as one might expect. This is found for the L_a excitations of BP, An, and DBAn. Et, as already pointed out, is a

Table 3. Numerical Comparison for $^3\Delta E$ and S/T Gaps for PBE, LC*, and CCSD(T)^a

		$^3\Delta E$			S/T gap		
		PBE	LC*	CCSD(T)	PBE	LC*	CCSD(T)
BP	L _a	2.38	2.44	2.82	0.99	1.53	1.28
	L _b	2.99	3.34	3.34	0.25	0.44	0.16
An	L _a	1.92	1.90	2.34	1.02	1.60	1.32
	L _b	3.34	3.62	3.52	0.30	0.36	0.06
DBAn	L _a	2.26	2.38	2.73	0.83	1.34	1.18
	L _b	2.95	3.29	3.35	0.27	0.52	0.22
CN9		1.68	1.31	1.92	1.79	2.09	0.86
Et		4.28	3.85	4.64	3.52	4.01	3.52
DMABN		3.05	3.15	3.54	1.26	1.65	1.18
Az	L _a	1.94	1.91	2.18	0.39	0.45	-0.24
	L _b	2.37	2.03	2.20	1.12	1.72	1.44
DANS		1.63	2.07	2.50	0.54	1.24	1.13
TCNE-B		1.33	3.11	3.61	0.02	0.02	0.08

^aAll values in electronvolts.

special case where the large magnitude of all integrals amplifies the difference between PBE and LC*.

It is interesting that the TDDFT triplet excitation energies for the H–L transitions of the “non-CT” π chromophores BP, An, and DBAn underestimate the wave function reference data severely, by ~ 0.4 to 0.5 eV. On the other hand, the PBE orbital energy gaps $\Delta\epsilon$ agree very well with the CCSD(T) triplet energies, and likewise for the CT-like candidates: Az, CN9, and DMABN. The $[ailf_{XC}^{\alpha\alpha}|ai]$ in the two-level model and involvement of other orbital pairs reduce the triplet excitation energy relative to the orbitals gap across all samples (the $[p\ q\ f_{XC}^{\sigma\sigma}|r\ s]$ integrals for the frontier orbitals are negative), unless they are very small due to orbital separation. Since the only positive term in the triplet energy, other than $\Delta\epsilon$ in eq 16b, is $-[ailf_{XC}^{\alpha\beta}|ai]$, this suggests that these contributions are too small when calculated with a semilocal approximate functional, or that $\Delta\epsilon$ is too small to begin with, or both.

The S/T separation appears to be overestimated by PBE in some cases and underestimated in others (except for TCNE-B where the S/T separation becomes negligible due to the pure long-range CT character of the excitations). Examples where the S/T separation is overestimated by PBE are CN9 (dramatically), Az (L_a, moderately; the CCSD(T) S/T gap is negative), An (L_b, moderately), DMABN (slightly), and DBAn (L_b, very slightly). The PBE triplet excitations are underestimated at the same time, which provides some error compensation for CN9 and Az. For DMABN the overestimation in the S/T gap is too small to correct for the 0.5 eV underestimation of the triplet energy by PBE. A strong overestimation of the S/T gap also goes along with an overestimation of the singlet excitations by LC*.

For the H–L transition of the non-CT candidates BP, An, and DBAn, the PBE S/T gap is underestimated by ~ 0.3 eV. As the triplet energies are already too low with PBE, the errors add up, and the singlet excitations are severely too low. The triplet energies obtained with the LC* functional are also too low and very similar to PBE, but the LC* S/T gaps are overestimated by roughly the same amount. The apparently good performance of LC* for these excitations can therefore be viewed as cases of error compensation. This situation is also found for other molecules: With LC*, all H–L triplet excitations are too low in energy, and all S/T gaps are too large.

Since the S/T gap is calculated here as the difference between the singlet and triplet energies, one can alternatively

attribute any problems with the H–L transitions of BP, An, and DBAn dominantly to the triplet energies, and consider the singlet energies with LC* correctly predicted for the right reasons. The S/T gap would then be too large simply because the triplet energies are too low. A possible reason for underestimated LC* triplet energies could be a triplet near-instability of the singlet reference, due to the overall large fraction of exact exchange in the functional.⁸⁶ Indeed, Peach and Tozer⁸⁷ noted recently that excitations involving orbitals with large spatial overlap tend to have triplet near-instabilities, and recommended using the Tamm–Danoff Approximation (TDA) as a remedy, in conjunction with a Coulomb-attenuated RS functional. On the other hand, the use of *tuned* LC functionals has been shown to reduce the severity of such errors significantly.⁸⁸ Furthermore, the comparison of BP, An, and DBAn with CN9 reveals very similar trends as far as the triplet energies and the impact of LC* on the S/T gap is concerned (rendering it more positive), which points to a lack of correlation contributions in the latter as a major potential source of error for singlet transitions. We also note that the usual TDDFT CT-problem adversely impacts singlet as well as triplet excitations, with concomitant low impact of the TDA for actual CT situations, which is very different from the CT-like scenarios.

We investigated the impact of the TDA on the excitation energies in the test set (see Table S10 and Figures S16 and S17 in the Supporting Information). For LC*, the calculated $^3\Delta E$ are increased and hence corrected toward CCSD(T). Slight to moderate increases are obtained for the $^1\Delta E$ excitations for most molecules, and the average deviation versus CCSD(T) increases from 0.04 eV (full-TDDFT LC*) to 0.22 eV (TDA LC*). With the PBE functional, the TDA has virtually no effect on the triplet excitation energies and also only causes small changes of the $^1\Delta E$. For CN9, the TDA substantially increases $^1\Delta E$, in particular, which severely worsens the agreement with CCSD(T).

We hesitate to attribute an apparent CT-like situation, namely, strong improvement of a singlet excitation by an LC functional, in particular when tuned, to the TDDFT CT problem. The latter exists, of course, as represented by DANS and TCNE-B in our test set of molecules. The dramatic improvements by the LC functional for cases such as BP, An, and DBAn, however, can also be attributed to a change in sign of the error of the S/T separation. Overall, differential

correlation between the excited state and the ground state appears to be a major issue. For some excitations, TDDFT with semilocal functionals suffers from compounding rather than compensating errors. The cyanine problem^{34,71} is that the S/T gap is already severely overestimated with semilocal functionals, and it gets worse when switching to hybrid functionals. The error for the cyanine appears to be driven to some extent by a large H–L exchange ERI, when measured relative to the corresponding Coulomb integral, entering the S/T gap along with a lack of sufficiently large negative correlation corrections from the XC response kernel.

Regarding the L_b transitions of some of the molecules in the test set, it can be noticed that BP, An, and DBAn afford particularly large differences between CCSD and CCSD(T) for the triplet excitations, more so than for the other transitions/molecules studied herein. The CC data did not flag these or other calculated excitations as having double excitation character. This reinforces the assessment that TDDFT may have a problem with the differential correlation between the ground and excited states for these molecules. The 3L_b energies of BP, An, and DBAn are underestimated by TDDFT/PBE, while the S/T gaps are mildly to moderately overestimated, providing some error compensation. The LC* triplet energies and S/T gaps are all higher than those from PBE, leading to too high 1L_b energies. The performance of LC* is here comparable with CCSD which, however, does not appear to be good enough. The global hybrid B3LYP offers the right compromise between PBE and LC* and gives reasonable energies for the 1L_b transitions. For Az, PBE and LC* are roughly 0.2 eV above and below the CCSD(T) 3L_b , respectively, while the S/T separation is 0.3 eV too small with PBE and 0.5 eV too high with LC*. In both cases, there is error compensation, and the 1L_b energies remain not too far from the CCSD(T) benchmark.

4. CONCLUSIONS

For a two-level model, a previously introduced CT-like criterion of the spatial overlap of the two auxiliary orbitals of eq 6 is equivalent to the integral over the half of the modulus of the electron density change upon excitation. Physical CT is indicated by large values of this integral. More generally, the $(1/2)\langle|\Delta\rho|\rangle$ integral is useful in detecting electron density changes involving spatially disjoint orbitals, no matter if the process takes place over a short or long distance. We find that a sizable value of the integral in conjunction with relatively large spatial overlaps of the orbital pairs involved can help identifying cases where differential correlation between the ground and excited state may be large and not well-predicted by TDDFT linear response calculations.

In comparison with CCSD(T), triplet energies are systematically too low with TDDFT—severely so in some cases. For some systems in the test set, there is also a large error in the S/T separation, which changes sign when going from PBE to the LC* functional. This gives the appearance of an improvement of the singlet excitation energy analogous to how LC* dramatically improves proper CT excitation energies. Assuming that the CCSD(T) data are accurate, however, there is little resemblance to an actual CT scenario. What appears to render CT-like cases qualitatively different from the cyanine problem is the sign of the error of the S/T separation at the non-hybrid level. As a working definition, one may choose to refer to singlet excitations whose energies are much too low with a non-hybrid functional and improve dramatically with a tuned LC

functional, similar to a proper CT excitation, as CT-like. In this case, one would consider the LC* calculations of the singlet excitations as performing good for the right reasons, while the sole problem would be triplet near-instabilities for the triplet excitations with concomitant much too low energies. However, conceptualizing CT-like excitations in this way may distract from an important problem, namely, the apparent inability of common approximate XC response kernels to generate sufficient correlation contributions to the excitation energy and the possibility of pronounced errors in the S/T separation.

Our analysis focused on intramolecular CT-like excitations with significant dipole strengths for the singlet transitions. The case of spurious intermolecular CT within dimers at large separation of the monomers,^{89–91} typically with low intensities, is different. We previously also noted problems with spurious CT between solvent and solute in TDDFT calculations of amino acids in water clusters with non-LC functionals.⁹² Such unphysical CT can lead to a breakdown of TDDFT calculations with non-hybrid functionals and global hybrids in calculations involving spatially separated molecules. LC functionals, and in particular tuned variants, greatly help to eliminate such transitions from TDDFT spectra, such that the performance for monomers and dimers is comparable.⁹¹ Even though no net CT may occur in the spurious intermolecular CT, the origin of the problem is closely related to the CT problem affecting physically meaningful excitations,⁸⁹ and therefore the improvements with LC functionals are obtained for the right reasons.

■ ASSOCIATED CONTENT

S Supporting Information

All integrals used in the analysis of the excitations (tables and plots). XYZ coordinates for all molecules. Additional CC data and additional CASPT2 data obtained with different basis sets and CAS spaces, along with assignments of the electronic excitations. Additional data related to the overlap criteria of Section 3.1. An alternative way of examining the auxiliary overlaps of Section 3.2 for the four-orbital sets of Az and An. The Supporting Information is available free of charge on the ACS Publications website at DOI: 10.1021/acs.jctc.5b00335.

■ AUTHOR INFORMATION

Corresponding Author

*E-mail: jochen@buffalo.edu.

Notes

The authors declare no competing financial interest.

■ ACKNOWLEDGMENTS

J.A. and B.M.II acknowledge support by the National Science Foundation, Grant No. CHE-1265833. J.A. thanks Prof. L. Kronik for constructive discussions on the topic of CT. H.S. is grateful for financial support by the China Scholarship Council. N.G. acknowledges support from the U.S. Department of Energy, Office of Science, Office of Advanced Scientific Computing Research, Scientific Discovery through Advanced Computing (SciDAC) program, under Award No. DE-SC0008666 for the analytical TDDFT excited-state gradients developments in NWChem. We thank the Center for Computational Research at the Univ. at Buffalo for providing and hosting computational resources. A portion of the calculations were performed at the Environmental Molecular Sciences Laboratory, a national scientific user facility sponsored by the Department of Energy's Office of Biological and

Environmental Research and located at the Pacific Northwest National Laboratory.

■ DEDICATION

¹In memory of Tom Ziegler who passed away unexpectedly in March 2015.

■ REFERENCES

- (1) Casida, M. E.; Gutierrez, F.; Guan, J.; Gadea, F.-X.; Salahub, D. R.; Daudey, J.-P. *J. Chem. Phys.* **2000**, *113*, 7062–7071.
- (2) Peach, M. J. G.; Benfield, P.; Helgaker, T.; Tozer, D. J. *J. Chem. Phys.* **2008**, *128*, 044118–8.
- (3) Kuritz, N.; Stein, T.; Baer, R.; Kronik, L. *J. Chem. Theory Comput.* **2011**, *7*, 2408–2415.
- (4) Guido, C. A.; Cortona, P.; Mennucci, B.; Adamo, C. *J. Chem. Theory Comput.* **2013**, *9*, 3118–3126.
- (5) Etienne, T.; Assfeld, X.; Monari, A. *J. Chem. Theory Comput.* **2014**, *10*, 3896–3905.
- (6) Etienne, T.; Assfeld, X.; Monari, A. *J. Chem. Theory Comput.* **2014**, *10*, 3906–3914.
- (7) Cohen, A. J.; Mori-Sánchez, P.; Yang, W. *Science* **2008**, *321*, 792–794.
- (8) Elliott, P.; Furche, F.; Burke, K. Excited States from Time-Dependent Density Functional Theory. In *Reviews in Computational Chemistry*; Lipkowitz, K. B., Cundari, T. R., Eds.; John Wiley & Sons, Inc.: Hoboken, NJ, 2009; pp 91–165.
- (9) Dreuw, A.; Weisman, J. L.; Head-Gordon, M. *J. Chem. Phys.* **2003**, *119*, 2943–2946.
- (10) Stein, T.; Kronik, L.; Baer, R. *J. Am. Chem. Soc.* **2009**, *131*, 2818–2820.
- (11) Autschbach, J. *ChemPhysChem* **2009**, *10*, 1757–1760.
- (12) Dreuw, A.; Fleming, G. R.; Head-Gordon, M. *Phys. Chem. Chem. Phys.* **2003**, *5*, 3247–3256.
- (13) Dreuw, A.; Head-Gordon, M. *J. Am. Chem. Soc.* **2004**, *126*, 4007–4016.
- (14) Neugebauer, J.; Gritsenko, O.; Baerends, E. J. *J. Chem. Phys.* **2006**, *124*, 214102–11.
- (15) Ziegler, T.; Seth, M.; Krykunov, M.; Autschbach, J.; Wang, F. J. *Mol. Struct. (special TDDFT issue of THEOCHEM)* **2009**, *914*, 106–109.
- (16) Rudolph, M.; Ziegler, T.; Autschbach, J. *J. Chem. Phys.* **2011**, *391*, 92–100.
- (17) Fabian, J. *Theor. Chem. Acc.* **2001**, *106*, 199–217.
- (18) Richard, R. M.; Herbert, J. M. *J. Chem. Theory Comput.* **2011**, *7*, 1296–1306.
- (19) Grimme, S.; Parac, M. *ChemPhysChem* **2003**, *5*, 292–295.
- (20) Lopata, K.; Reslan, R.; Kowalska, M.; Neuhauser, D.; Govind, N.; Kowalski, K. *J. Chem. Theory Comput.* **2011**, *7*, 3686–3693.
- (21) Wong, B. M.; Hsieh, T. H. *J. Chem. Theory Comput.* **2010**, *6*, 3704–3712.
- (22) Goerigk, L.; Grimme, S. *J. Chem. Theory Comput.* **2011**, *7*, 3272–3277.
- (23) Arulmozhiraja, S.; Coote, M. L. *J. Chem. Theory Comput.* **2012**, *8*, 575–584.
- (24) Krykunov, M.; Grimme, S.; Ziegler, T. *J. Chem. Theory Comput.* **2012**, *8*, 4434–4440.
- (25) Yanai, T.; Tew, D. P.; Handy, N. C. *Chem. Phys. Lett.* **2004**, *393*, 51–57.
- (26) Kronik, L.; Stein, T.; Refaeli-Abramson, S.; Baer, R. *J. Chem. Theory Comput.* **2012**, *8*, 1515–1531.
- (27) Baer, R.; Livshits, E.; Salzner, U. *Annu. Rev. Phys. Chem.* **2010**, *61*, 85–109.
- (28) Srebro, M.; Autschbach, J. *J. Phys. Chem. Lett.* **2012**, *3*, 576–581.
- (29) Jacquemin, D.; Moore, B. II.; Planchat, A.; Adamo, C.; Autschbach, J. *J. Chem. Theory Comput.* **2014**, *10*, 1677–1685.
- (30) Sun, H.; Autschbach, J. *J. Chem. Theory Comput.* **2014**, *10*, 1035–1047.
- (31) Refaeli-Abramson, S.; Sharifzadeh, S.; Govind, N.; Autschbach, J.; Neaton, J. B.; Baer, R.; Kronik, L. *Phys. Rev. Lett.* **2012**, *109*, 226405–5.
- (32) Stein, T.; Autschbach, J.; Govind, N.; Kronik, L.; Baer, R. *J. Phys. Chem. Lett.* **2012**, *3*, 3740–3744.
- (33) Sun, H.; Autschbach, J. *ChemPhysChem* **2013**, *14*, 2450–2461.
- (34) Moore, B. II.; Autschbach, J. *J. Chem. Theory Comput.* **2013**, *9*, 4991–5003.
- (35) Geertsen, J.; Rittby, M.; Bartlett, R. *Chem. Phys. Lett.* **1989**, *164*, 57–62.
- (36) Comeau, D.; Bartlett, R. *Chem. Phys. Lett.* **1993**, *207*, 414–423.
- (37) Stanton, J. F.; Bartlett, R. *J. J. Chem. Phys.* **1993**, *98*, 7029–7039.
- (38) Kowalski, K.; Piecuch, P. *Chem. Phys. Lett.* **2001**, *347*, 237–246.
- (39) Hirata, S. *J. Chem. Phys.* **2004**, *121*, 51–59.
- (40) Frisch, M. J.; Trucks, G. W.; Schlegel, H. B.; Scuseria, G. E.; Robb, M. A.; Cheeseman, J. R.; Scalmani, G.; Barone, V.; Mennucci, B.; Petersson, G. A.; Nakatsuji, H.; Caricato, M.; Li, X.; Hratchian, H. P.; Izmaylov, A. F.; Bloino, J.; Zheng, G.; Sonnenberg, J. L.; Hada, M.; Ehara, M.; Toyota, K.; Fukuda, R.; Hasegawa, J.; Ishida, M.; Nakajima, T.; Honda, Y.; Kitao, O.; Nakai, H.; Vreven, T.; Montgomery, J. A. Jr.; Peralta, J. E.; Ogliaro, F.; Bearpark, M.; Heyd, J. J.; Brothers, E.; Kudin, K. N.; Staroverov, V. N.; Kobayashi, R.; Normand, J.; Raghavachari, K.; Rendell, A.; Burant, J. C.; Iyengar, S. S.; Tomasi, J.; Cossi, M.; Rega, N.; Millam, J. M.; Klene, M.; Knox, J. E.; Cross, J. B.; Bakken, V.; Adamo, C.; Jaramillo, J.; Gomperts, R.; Stratmann, R. E.; Yazyev, O.; Austin, A. J.; Cammi, R.; Pomelli, C.; Ochterski, J. W.; Martin, R. L.; Morokuma, K.; Zakrzewski, V. G.; Voth, G. A.; Salvador, P.; Dannenberg, J. J.; Dapprich, S.; Daniels, A. D.; Farkas, O.; Foresman, J. B.; Ortiz, J. V.; Cioslowski, J.; Fox, D. J. *Gaussian 09*, Revision A.02; Gaussian, Inc.: Wallingford, CT, 2009. <http://www.gaussian.com/>. Accessed 05/2015.
- (41) Becke, A. D. *J. Chem. Phys.* **1993**, *98*, 5648–5652.
- (42) Lee, C.; Yang, W.; Parr, R. G. *Phys. Rev. B* **1988**, *37*, 785–789.
- (43) Dunning, T. H., Jr. *J. Chem. Phys.* **1989**, *90*, 1007.
- (44) Hariharan, P. C.; Pople, J. A. *Theor. Chim. Acta* **1973**, *28*, 213.
- (45) Franch, M. M.; Pietro, W. J.; Hehre, W. J.; Binkley, J. S.; Gordon, M. S.; Defrees, D. J.; Pople, J. A. *J. Chem. Phys.* **1982**, *77*, 3654–3665.
- (46) Kowalski, K.; Piecuch, P. *J. Chem. Phys.* **2004**, *120*, 1715–1738.
- (47) Weigend, F.; Ahlrichs, R. *Phys. Chem. Chem. Phys.* **2005**, *7*, 3295–3305.
- (48) Schuchardt, K. L.; Didier, B. T.; Elsethagen, T.; Sun, L.; Gurumoorthy, V.; Chase, J.; Li, J.; Windus, T. L. *J. Chem. Inf. Model.* **2007**, *47*, 1045–1052.
- (49) Valiev, M.; Bylaska, E. J.; Govind, N.; Kowalski, K.; Straatsma, T. P.; Dam, H. J. V.; Wang, D.; Nieplocha, J.; Apra, E.; Windus, T. L.; de Jong, W. A. *Comput. Phys. Commun.* **2010**, *181*, 1477–1489.
- (50) Bylaska, E. J.; de Jong, W. A.; Govind, N.; Kowalski, K.; Straatsma, T. P.; Valiev, M.; van Dam, J. J.; Wang, D.; Apra, E.; Windus, T. L.; Hammond, J.; Autschbach, J.; Aquino, F.; Nichols, P.; Hirata, S.; Hackler, M. T.; Zhao, Y.; Fan, P.-D.; Harrison, R. J.; Dupuis, M.; Smith, D. M. A.; Glaesemann, K.; Nieplocha, J.; Tipparaju, V.; Krishnan, M.; Vazquez-Mayagoitia, A.; Jensen, L.; Swart, M.; Wu, Q.; van Voorhis, T.; Auer, A. A.; Nooijen, M.; Crosby, L. D.; Brown, E.; Cisneros, G.; Fann, G. I.; Frucht, H.; Garza, J.; Hirao, K.; Kendall, R.; Nichols, J. A.; Tsemekhman, K.; Wolinski, K.; Anchell, J.; Bernholdt, D.; Borowski, P.; Clark, T.; Clerc, D.; Dachs, H.; Deegan, M.; Dyall, K.; Elwood, D.; Glendening, E.; Gutowski, M.; Hess, A.; Jaffe, J.; Johnson, B.; Ju, J.; Kobayashi, R.; Kutteh, R.; Lin, Z.; Littlefield, R.; Long, X.; Meng, B.; Nakajima, T.; Niu, S.; Pollack, L.; Rosing, M.; Sandrone, G.; Stave, M.; Taylor, H.; Thomas, G.; van Lenthe, J.; Wong, A.; Zhang, Z. *NWChem*, A Computational Chemistry Package for Parallel Computers, Version 6 (2012 developer's version); Pacific Northwest National Laboratory: Richland, WA, 2012.
- (51) Perdew, J. P.; Burke, K.; Ernzerhof, M. *Phys. Rev. Lett.* **1998**, *80*, 891.
- (52) Srebro, M.; Autschbach, J. *J. Chem. Theory Comput.* **2012**, *8*, 245–256.
- (53) Clark, T.; Chandrasekhar, J.; Spitznagel, G. W.; v.R. Schleyer, P. *J. Comput. Chem.* **1983**, *4*, 294–301.

- (54) Levy, M.; Perdew, J. P.; Sahni, V. *Phys. Rev. A* **1984**, *30*, 2745–2748.
- (55) Livshits, E.; Baer, R. *Phys. Chem. Chem. Phys.* **2007**, *9*, 2932–2941.
- (56) Karolewski, A.; Kronik, L.; Kümmel, S. *J. Chem. Phys.* **2013**, *138*, 204115–11.
- (57) Tamblyn, I.; Refaelly-Abramson, S.; Neaton, J. B.; Kronik, L. *J. Phys. Chem. Lett.* **2014**, *5*, 2734–2741.
- (58) Autschbach, J.; Srebro, M. *Acc. Chem. Res.* **2014**, *47*, 2592–2602.
- (59) Silverstein, D. W.; Govind, N.; van Dam, H. J. J.; Jensen, L. *J. Chem. Theory Comput.* **2013**, *9*, 5490–5503.
- (60) Aquilante, F.; De Vico, L.; Ferré, N.; Ghigo, G.; Malmqvist, P.; Neogrady, P.; Pedersen, T. B.; Pitoňák, M.; Reiher, M.; Roos, B. O.; Serrano-Andrés, L.; Urban, M.; Veryazov, V.; Lindh, R. *J. Comput. Chem.* **2010**, *31*, 224–247.
- (61) Baerends, E. J.; Ziegler, T.; Autschbach, J.; Bashford, D.; Bérces, A.; Bickelhaupt, F. M.; Bo, C.; Boerrigter, P. M.; Cavallo, L.; Chong, D. P.; Deng, L.; Dickson, R. M.; Ellis, D. E.; van Faassen, M.; Fan, L.; Fischer, T. H.; Fonseca Guerra, C.; Ghysels, A.; Giannoni, A.; van Gisbergen, S. J. A.; Götz, A. W.; Groeneveld, J. A.; Gritsenko, O. V.; Grüning, M.; Gusarov, S.; Harris, F. E.; van den Hoek, P.; Jacob, C. R.; Jacobsen, H.; Jensen, L.; Kaminski, J. W.; van Kessel, G.; Kootstra, F.; Kovalenko, A.; Krykunov, M. V.; van Lenthe, E.; McCormack, D. A.; Michalak, A.; Mitoraj, M.; Neugebauer, J.; Nicu, V. P.; Noddleman, L.; Osinga, V. P.; Patchkovskii, S.; Philipsen, P. H. T.; Post, D.; Pye, C. C.; Raveneck, W.; Rodríguez, J. I.; Ros, P.; Schipper, P. R. T.; Schreckenbach, G.; Seldenthuis, J. S.; Seth, M.; Snijders, J. G.; Solà, M.; Swart, M.; Swerhone, D.; te Velde, G.; Vernooij, P.; Versluis, L.; Visscher, L.; Visser, O.; Wang, F.; Wesolowski, T. A.; van Wezenbeek, E. M.; Wiesenekker, G.; Wolff, S. K.; Woo, T. K.; Yakovlev, A. L. *Amsterdam Density Functional*, SCM; Vrije Universiteit: Amsterdam, The Netherlands, URL <http://www.scm.com>. Accessed 05/15.
- (62) Vosko, S. H.; Wilk, L.; Nusair, M. *Can. J. Phys.* **1980**, *58*, 1200–1211.
- (63) Gritsenko, O.; Baerends, E. *J. J. Chem. Phys.* **2004**, *121*, 655–660.
- (64) Kronik, L.; Stein, T.; Refaelly-Abramson, S.; Baer, R. *J. Chem. Theory Comput.* **2012**, *8*, 1515–1531.
- (65) Tawada, Y.; Tsuneda, T.; Yanagisawa, S.; Yanai, T.; Hirao, K. *J. Chem. Phys.* **2004**, *120*, 8425–8433.
- (66) Lange, A. W.; Rohrdanz, M. A.; Herbert, J. M. *J. Phys. Chem. B* **2008**, *112*, 6304–6308.
- (67) Wang, Y.; Wu, G. *Int. J. Quantum Chem.* **2008**, *108*, 430–439.
- (68) Serrano-Andrés, L.; Merchán, M.; Nebot-Gil, I.; Lindh, R.; Roos, B. O. *J. Chem. Phys.* **1993**, *98*, 3151–3162.
- (69) Wiberg, K. B.; de Oliveira, A. E.; Trucks, G. *J. Phys. Chem. A* **2002**, *106*, 4192–4199.
- (70) Send, R.; Valsson, O.; Filippi, C. *J. Chem. Theory Comput.* **2011**, *7*, 444–455.
- (71) Le Guennic, B.; Jacquemin, D. *Acc. Chem. Res.* **2015**, *48*, 530–537.
- (72) Perkampus, H. *UV-Vis Atlas of Organic Compounds*; VCH: Weinheim, Germany, 1992; p 705.
- (73) Falden, H. H.; Falster-Hansen, K. R.; Bak, K. L.; Rettrup, S.; Sauer, S. P. *A. J. Phys. Chem. A* **2009**, *113*, 11995–12012.
- (74) Bulliard, C.; Allan, M.; Wirtz, G.; Haselbach, E.; Zachariasse, K. A.; Detzer, N.; Grimme, S. *J. Phys. Chem. A* **1999**, *103*, 7766–7772.
- (75) Schreiber, M.; Buß, V.; Fülscher, M. P. *Phys. Chem. Chem. Phys.* **2001**, *3*, 3906–3912.
- (76) Champagne, B.; Guillaume, M.; Zuterman, F. *Chem. Phys. Lett.* **2006**, *425*, 105–109.
- (77) Grimme, S.; Neese, F. *J. Chem. Phys.* **2007**, *127*, 154116.
- (78) Jacquemin, D.; Zhao, Y.; Valero, R.; Adamo, C.; Ciofini, I.; Truhlar, D. G. *J. Chem. Theory Comput.* **2012**, *8*, 1255–1259.
- (79) Fabian, J. *Dyes Pigm.* **2010**, *84*, 36–53.
- (80) Filatov, M.; Huix-Rotllant, M. *J. Chem. Phys.* **2014**, *141*, 024112.
- (81) Boulanger, P.; Chibani, S.; Le Guennic, B.; Duchemin, I.; Blase, X.; Jacquemin, D. *J. Chem. Theory Comput.* **2014**, *10*, 4548–4556.
- (82) Zhekova, H.; Krykunov, M.; Autschbach, J.; Ziegler, T. *J. Chem. Theory Comput.* **2014**, *10*, 3299–3307.
- (83) Masunov, A. E. *Int. J. Quantum Chem.* **2010**, *110*, 3095–3100.
- (84) Rosa, A.; Ricciardi, G.; Gritsenko, O.; Baerends, E. J. Excitation energies of metal complexes with time-dependent density functional theory. In *Principles and Applications of Density Functional Theory in Inorganic Chemistry I*; Kaltsoyannis, N., McGrady, J. E., Eds.; Springer: Heidelberg, Germany, 2004; Vol. 112, pp 49–115.
- (85) Ziegler, T. *J. Chem. Soc., Dalton Trans.* **2002**, 642–652.
- (86) Peach, M. J. G.; Williamson, M. J.; Tozer, D. J. *J. Chem. Theory Comput.* **2011**, *7*, 3578–3585.
- (87) Peach, M. J. G.; Tozer, D. J. *J. Phys. Chem. A* **2012**, *116*, 9783–9789.
- (88) Sears, J. S.; Koerzdoerfer, T.; Zhang, C.-R.; Bredas, J.-L. *J. Chem. Phys.* **2011**, *135*, 151103.
- (89) Hieringer, W.; Görling, A. *Chem. Phys. Lett.* **2006**, *419*, 557–562.
- (90) Phillips, H.; Geva, E.; Dunietz, B. D. *J. Chem. Theory Comput.* **2012**, *8*, 2661–2668.
- (91) Moore, B., II; Autschbach, J. *ChemistryOpen* **2012**, *1*, 184–194.
- (92) kundrat, M. D.; Autschbach, J. *J. Chem. Theory Comput.* **2008**, *4*, 1902–1914.